

Space-Air-Ground-Sea Integrated Networks: Modeling and Coverage Analysis

Jiajie Xu¹, Graduate Student Member, IEEE, Mustafa A. Kishk², Member, IEEE, and Mohamed-Slim Alouini³, Fellow, IEEE

Abstract—Due to its potential to enable global connectivity in remote locations, such as rural areas and islands, Space-Air-Ground networks have become an ambitious solution for terrestrial communication in the sixth generation (6G) wireless communication network. In this paper, we propose a novel structure of Space-Air-Ground-Sea integrated networks (SAGSINs) to study and derive the coverage probability (CP) of users who are annotated as surface stations (SSs) on the far-reaching ocean surface that is far away from the coastline. By incorporating different types of relays such as onshore stations (OSs), tethered balloons (TBs), high altitude platforms (HAPs), and satellites (SATs), communication links between the terrestrial core connected base stations (CCBSs) and SSs are established via one of the four types of relay stations. Considering practical scenarios with a random distribution of SSs, we model the channel using the point-to-area model, which is recommended by ITU (for OSs to SS), the Rician model (for TBs or HAPs to SS), and the Shadowed-Rician model (for SATs to SS). When the SS's distance from the coastline continues to increase from zero, since different channel models are considered, different relay stations will result in specific received signal strengths at SSs. The most powerful relay station will be chosen as the relay at one time. Hence, as we move away from the coastline, the respective strengths of the different types of relay stations vary, and hence, the association preference (among HAPs, OSs, TBs, and SATs) of the SSs changes leading to a CP value high enough even at locations far away from the coastline into the ocean. We analyze the CP using tools from stochastic geometry. Comparisons of CP between the integrated system with four types of relay stations and the single relay station system (only one type of relay station available) are represented. Numerical results verified by Monte-Carlo simulations reveal insights into the applicability of SAGSINs.

Index Terms—Space-air-ground-sea integrated networks, maritime communication, stochastic geometry, coverage probability.

I. INTRODUCTION

A. Motivation

THE fifth-generation (5G) cellular communication networks are getting standardized and more mature in recent years, but remote locations such as rural areas, islands, and

Manuscript received 5 August 2022; revised 26 November 2022 and 22 January 2023; accepted 27 January 2023. Date of publication 7 February 2023; date of current version 12 September 2023. This work was supported by the KAUST Office of Sponsored Research. The associate editor coordinating the review of this article and approving it for publication was S. Zhou. (Corresponding author: Mustafa A. Kishk.)

Jiajie Xu and Mohamed-Slim Alouini are with the Computer, Electrical, and Mathematical Science and Engineering Division, King Abdullah University of Science and Technology, Thuwal 23955-6900, Saudi Arabia (e-mail: jiajie.xu.1@kaust.edu.sa; slim.alouini@kaust.edu.sa).

Mustafa A. Kishk is with the Department of Electronic Engineering, Maynooth University, Maynooth, W23 F2H6 Ireland (e-mail: mustafa.kishk@mu.ie).

Color versions of one or more figures in this article are available at <https://doi.org/10.1109/TWC.2023.3241341>.

Digital Object Identifier 10.1109/TWC.2023.3241341

end-users in the far-reaching ocean surface still can not be connected. A lot of literature in research on 6G wireless networks, to name a few [1], [2], [3], [4], [5], focus on Space-Air-Ground integrated networks (SAGINs) and attempt to build a globally integrated network.

It is well known that 71% of the earth is covered by water, and most transnational cargo transportation is done over the sea. Added to the rapid development of ocean exploration, a network that can cover a large-scale and far-reaching ocean has become an urgent need in order to provide connectivity for ships and connected underwater systems. Developed from SAGINs, Space-Air-Ground-Sea integrated networks (SAGSINs) have become a promising solution for global connection and are capable of covering a large-scale and far-reaching ocean surface and even for underwater applications [6].

The existing literature focus on offshore communications [7], [8], which can cover sea-surface applications within at most 100 kilometers away from the coastline. But for the devices, stations, and users farther from the coastline, the connection is unavailable. Undoubtedly, Low Earth Orbit (LEO) satellites can achieve global connectivity [9], [10], but the disadvantages of long latency, low data rate, and unstable connection greatly restrict the explorations with higher requirements in large-scale and far-reaching ocean, such as marine environmental monitoring or underwater communication [11], [12] achieved by Underwater Internet of Things (UIoT), underwater terrain exploration or mapping [13] executed by autonomous underwater vehicle (AUV), underwater sensor and communication systems for target detection and tracking [14], to name a few [15], [16], [17], [18], where all of these applications require a high data rate and stable communication between surface stations or end-users and terrestrial core connected base station (CCBS). Motivated by the requirements of wireless communication in a large-scale and far-reaching ocean, a Space-Air-Ground-Sea integrated network is proposed to provide a reliable connection to applications in a large-scale ocean, for example, fishing boats in various marine fishing areas, offshore oil/gas drilling platforms, transoceanic freighters, and marine environment monitoring base stations, etc. In this paper, the SAGSIN structure with four different types of relay stations, including OS, TB, HAP, and SAT, is proposed, and its CP for surface stations/users is analyzed.

B. Practical Implementation of SAGSIN

In this paper, we propose a communication structure of Space-Air-Ground-Sea integrated networks (SAGSINs), aimed

at wireless communication over the sea or underwater in a large area such as the Atlantic Ocean, the Pacific Ocean, the Indian Ocean, and so on. Considering the practical implementations or application scenarios for SAGSIN, communication is required between the inland stations to some offshore oil rigs, which are hundreds of kilometers from the coast. Communication links can be established, and unmanned systems can be built in the future. Besides that, unmanned systems can also be built in offshore wind farms. Marine fisheries are an important economic activity in many countries, and SAGSIN can provide a better communication performance to the large fishing boats in the Atlantic and the Pacific. Regarding the underwater application scenarios, SAGSIN can be used to connect to the underwater stations placed along with the underwater oil pipelines and fiber cables, which can monitor the oil pipelines and fiber cables and provide information in time in case of damage.

C. Related Work

Whether it is an underwater wireless sensor network, an autonomous underwater vehicle, a marine robot, a sea surface station, or an unmanned surface vehicle, a stable communication link is required between the user (on the surface or underwater) and the terrestrial stations. This link requires a non-terrestrial (aerial or space) station to act as a relay. Authors in [5], [19], [20], [21] explore the development of future communication networks from different perspectives, such as machine learning-assisted wireless networks, integrated networks paying more attention to the marine communication, etc. All of the work implies the need for integrated network research.

Besides that, the urgent need for SAGSINs comes from the basic fact that the covered range of ground-station-based networks is limited to about 15 km away from the coastline. In [7], land-to-ship measurements show that destructive and constructive interferences exist within a communication distance of 200~500 m. Near sea-surface communications are executed in [8] with a maximum route distance of 10 km. In [22], authors simulate a system composed of land stations that are designed to provide maritime wireless communication for ocean ships, including large ships and small ships. The large ships form a backbone mesh network that can provide network connections for themselves and smaller ships nearby. Authors in [23] perform experiments between a mobile single-antenna ship-borne transmitter and a fixed terrestrial receiver over the sea surface, and the communication distance extended from 15 km to 45 km. In [24], long-range (LR) Wi-Fi extends the connectivity to 60 km over the oceans using heterogeneous networks and relay nodes. Authors in [25] propose to build a broadband and broadcast/multicast maritime communication network to enhance the CP of the ocean of things. In this paper, shore towers, insular towers, and seaborne floating towers are included providing a hybrid communication link, and the concepts of “one-to-one” and “one-to-all” are quite suitable for a regional application scenario. However, for the coverage capacity of thousands of kilometers over the sea, the cost of the network needs to be further considered.

Aerial stations can act as relay stations to provide connectivity to the users on the sea surface. Considering the unmanned aerial vehicles (UAV) assisted mobile relay communication is limited by the capacity of wireless backhaul link between the UAV and the ground station, authors in [26] propose a caching UAV-assisted decode-and-forward relay communication and the semi-closed-form expression of the UAV’s optimal placement was derived for one single user. In this paper, the advantages and optimizable characteristics (in the horizontal direction) of mobile aerial relay stations are well studied. Work in [27] considers a scenario in which the offshore communication range is highly dependent on the height of the communication nodes. Hence, a position control approach for airborne multi-hop networks is proposed to take full advantage of the signal reflections on the sea surface. In this paper, different coverage performances related to different heights of the relays are revealed. Combining the research of [26] and [27], it is easy to understand that we can design an integrated network considering the directions of horizontal and vertical to achieve a better coverage performance. In [28], field tests made by the Norwegian university of science and technology demonstrate the feasibility of UAV providing communication connections to AUV (the AUV was on the sea surface).

Satellites can also provide connectivity to the users on the sea surface. As early as 1989 [29], Japanese scientists conducted satellite-based communications between ship stations and ground stations, and the data rate was 64 kbps. In [9], [30], [31], a survey about maritime Internet of Things based on satellite-terrestrial communication networks shows that the one-way transmission delays up to 270 ms and 40 ms for GEO and LEO. Chinese first mobile satellite communications system, Tiantong-1, as China’s first mobile satellite communications system can provide voice, short message, and low-speed data services, with a peak rate of 9.6 kbps. High throughput is achieved by satellite EchoStar-19. However, satellite-based communications are easily affected by climate and the marine environment, resulting in low reliability. Work in [32] provides an overview of the space-based network for maritime surveillance based on information sharing and evaluates the CP. Reference [32] shows the cognitive relay-based architecture for satellite-to-ground communication with a multi-band spectrum sensing operating on both free-space optical and radio frequency bands is available. It means that the structure of multiple aerial relay stations is feasible. Works on maritime Internet of Things can also be found in [33], [34], [35].

D. Contributions

In this paper, to provide stable and high-speed communication for maritime applications over large-scale and far-reaching oceans, a novel SAGSIN architecture is proposed. The contributions of this paper can be summarized as follows.

- *The proposed SAGSIN introduces a cooperative communication structure between the CCBSs and SSs considering a realistic and generic scenario.* Considering the different advantages and disadvantages of different types of relay stations, this work is the first to combine multiple

relays and attempt to cover an extended area over the sea at large distances from the shoreline. Four different types of relay stations (OS, TB, HAP, SAT) can be selected and associated in order to achieve stable and high-speed communication.

- *A more accurate model is established, assisted with multiple channel models and consideration of the randomness of the relays and SSs.* Considering the realistic propagation environment, different channels are applied in the ground-sea surface, the air-sea surface, and the space-sea surface links, including the channel recommended by ITU (for OS to SS), Rician channel (for TB or HAP to SS), and Shadowed-Rician channel (for SAT to SS). Tools from stochastic geometry are used to model the randomness of the four different types of relay stations and SSs. Besides that, interference that comes from the same tier of the relay station is analyzed.
- *A clear and accurate analytical framework is built, which helps to raise some insights into practical application.* Based on the constructed framework of SAGSIN, we analyze the association probability between the SS and each type of relay station for different values of the distance between the SS and the coastline. CP is analyzed considering the interference that comes from the same tier of the relay station. The analytical framework evaluated in this paper serves as a solid foundation and powerful tool for future research of SAGSIN and provides a necessary reference for maritime communication in large-scale and far-reaching oceans.

The remainder of this article is organized as follows. In section II, we detail the system model of the SAGSIN considered with the different channels and several key assumptions. Distance distributions between SS and different relay stations are calculated in section III. Then, we carry out CP analysis in section IV, calculating the final expression of CP for surface end-users or stations in large-scale and far-reaching oceans. Numerical results generated by Monte-Carlo simulations are illustrated in section V to corroborate our CP analysis and insights. Finally, section VI concludes this article.

II. SYSTEM MODEL

A. System Architecture

Different from the single relay communication structure between the sea-surface device and terrestrial core-connected base stations (CCBS), we propose to build an integrated network between CCBS and surface stations (SSs). We know that the coverage range of an aerial station is related to its height (which will be explained mathematically in the next Section). In order to achieve a non-gap coverage range, we need aerial relay stations with different heights. Hence, we can have choices of onshore stations (OSs), unmanned aerial vehicles (UAVs), tethered balloons (TBs), low altitude platforms (LAPs), high altitude platforms (HAPs), and satellites (SATs). Considering the limitation of energy and coverage performance, a proposed SAGSIN is shown in Fig. 1. In this figure, we have four different types of relay stations: onshore stations (OSs), tethered balloons (TBs), high altitude platforms

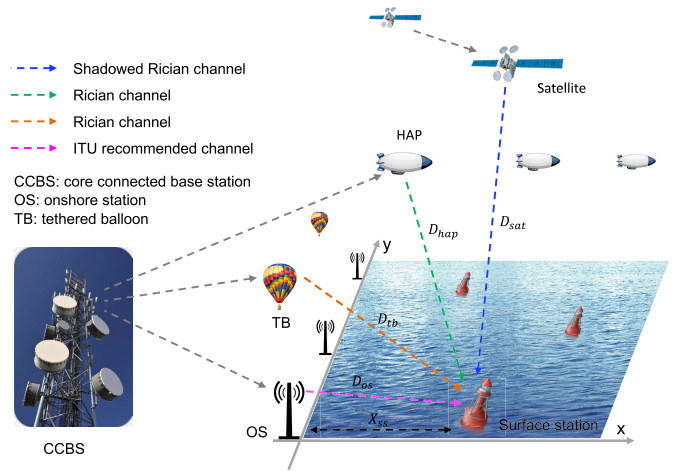


Fig. 1. SAGSIN communication system.

(HAPs), and satellites (SATs), to provide a better communication link between SSs and CCBSs in different ranges of the distance between the SS and the coastline. Although, each single relay station can act as the relay station alone between CCBS and SS. However, as the distance between the SS and the coastline increase, the four different types of relay stations will achieve the best communication performance in turn.

As shown in Fig. 1, we have different channel models between the SS and the four considered types of relay stations, which are inspired by existing literature [36], [37]. Distances between SS and four relay stations are also marked as D_{os} , D_{tb} , D_{hap} , D_{sat} . X_{ss} is the distance between the SS and the coastline. We can assume that the relay stations (for example, OSs) are placed in a two-dimensional area on the ground. However, when the SS chooses its target relay from the tier of OS, only the nearest OS will be selected (which must be close to the coastline), and the OSs far away from the coastline will most commonly be ignored. In this way, we can expect that all the potential target OSs are close to the coastline. So, we can assume the relay stations are subject to a one-dimensional Poisson Point Process (1D-PPP) along with the coastline (y -axis). Finally, the grey arrows mean communication links between the CCBS and the four types of relays. Since we are focusing on the downlink between the SSs and the four different types of relays, so it will not be considered in this paper.

We use tools from stochastic geometry to model the locations of the four types of relay stations as well as the SSs, as shown in Fig. 2. In the considered model, the coastline denotes the y -axis, the x -axis is perpendicular to the coastline with its positive direction toward the sea, and the z -axis is perpendicular to sea level. We perform our analysis for a given x coordinate (distance from the coastline) of the SS, X_{ss} . OSs and TBs are placed over the coastline, so the x coordinates of OS and TB, X_{os} , X_{tb} , are 0. X_{hap} is the distance between the HAP and the coastline. On the y -axis, SS, OS, TB, and HAP are modeled as 1D-PPPs with given densities γ_{os} , γ_{tb} , γ_{hap} . On the z -axis, the heights of SS, OS, TB, and HAP are noted as h_{ss} , h_{os} , h_{tb} , h_{hap} , and all of them are known. Therefore,

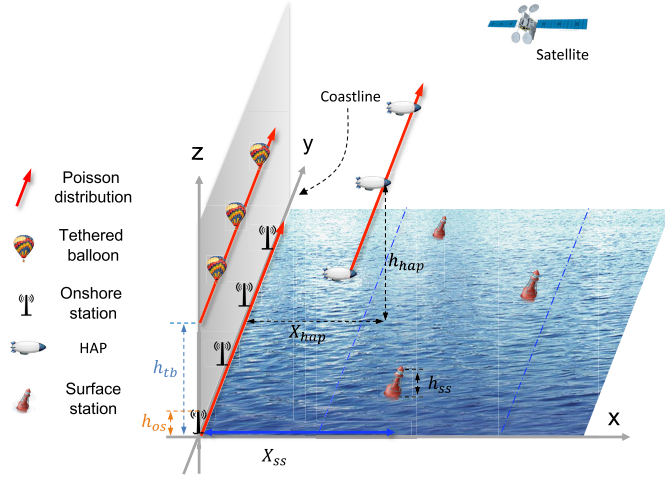


Fig. 2. Distribution model of each relay station and SS.

the Euclidean distance between the SS and the relay station (for example, OS) can be represented as

$$D_{os} = \sqrt{(X_{ss} - X_{os})^2 + Y_{os}^2 + (h_{os} - h_{ss})^2}, \quad (1)$$

where Y_{os} is subjects to 1D-PPP distribution.

Besides that, some critical aspects of the proposed SAGSIN should be clarified.

- In communication, due to relay stations in different tiers (OS or TB or HAP, or SAT) using different spectrums, there will be no intra-interference from different types of relays. For each tier of the relay station, the spectrum is divided into multiple sub-frequencies, and each sub-frequency can be occupied by one SS.
- At one time, a SS can connect to one relay station, but a relay station can connect to multiple SSs with different sub-frequencies. A SS connects to its selected relay station (in the tier with the highest association probability), which should be the nearest relay station in the tier. In this event, the relay station is regarded as a tagged station, and the SS is regarded as the target SS.
- All of the other relay stations in the same tier as the tagged station and using the same sub-frequency to communicate with other SSs are regarded as interference at the target SS.

B. Channel Models

For different types of relay stations, different channel models are applied. For OSs, the International Telecommunication Union (ITU) gives the recommended channel model to describe point-to-area communication. For TB and HAP, communication links between them and SS are similar, and the Rician channel model is applied, which is widely used in literature. The Shadowed-Rician channel will be applied for SATs to SSs communication.

1) *Channel Between SSs and OSs:* As recommended by ITU, for point-to-area communication with a frequency range from 30 MHz to 4000 MHz, the channel model is widely used for terrestrial and offshore wireless communication [6], [31]

and is shown as follows.

$$E(d) = \begin{cases} 106.9 - 20 \log\left(\frac{d}{1000}\right) + 2.38\left(1 - \exp\left(-\frac{d}{8940}\right)\right) \log\left(\frac{50}{t}\right), & d \geq 1000 \text{ m} \\ 106.9 - 20 \log(d_{inf}) + \frac{(E_{sup} - 106.9 + 20 \log(d_{inf})) \log\left(\frac{d_{slope}(d)}{d_{inf}}\right)}{\log\left(\frac{d_{sup}}{d_{inf}}\right)}, & 40 < d < 1000 \text{ m} \\ 106.9 - 20 \log\left(\sqrt{\frac{d^2 + (h_{os} - h_{ss})^2}{10^6}}\right), & d \leq 40 \text{ m} \end{cases}$$

where $E(d)$ with the unit of $\text{dB}(\mu\text{V}/\text{m})$,

$$\begin{cases} d_{inf} = \sqrt{(0.04)^2 + 10^{-6}(h_{os} - h_{ss})^2} \\ d_{sup} = \sqrt{1^2 + 10^{-6}(h_{os} - h_{ss})^2} \\ d_{slope}(d) = \sqrt{(d/1000)^2 + 10^{-6}(h_{os} - h_{ss})^2}, \end{cases} \quad (2)$$

and $E_{sup} = E(1000)$, d is the propagation distance in meters, t is the percentage time, and it will be regarded as 1 [36]. Hence, the basic transmission loss equivalent to a given field strength is given by:

$$\begin{aligned} L_{ITU}(d) &= -139.3 + E(d) - 20 \log\left(\frac{f}{10^6}\right) \text{ dB} \\ &= 10^{0.1(-139.3 + E(d) - 20 \log(f/10^6))}, \end{aligned} \quad (3)$$

where $L_{ITU}(d)$ is the transmission loss, $E(d)$ is the field strength for 1 kW effective radiated power (e.r.p.) in $\text{dB}(\mu\text{V}/\text{m})$, f is the frequency in Hz. So, the received power through ITU recommended channel is

$$P_r = P_t 10^{0.1(-139.3 + E(d) - 20 \log(f/10^6))} g_t g_r, \quad (4)$$

where g_t is the transmit antenna gain, g_r is the receive antenna gain.

2) *Channel Model Between TBs or HAPs and SSs:* The Channel model between TB or HAP and SSs is regarded as Rician channel [38], and shown as follows:

$$P_r = H g_t g_r, \quad (5)$$

where g_t and g_r are transmitter antenna gain and receiver antenna gain, H is the received signal power, and $H = g(A) = \frac{A^2}{2}$, where A is the envelope of the received signal passed the Rician channel, and we have

$$f_A(a) = \frac{a}{\sigma^2} \exp\left(-\frac{a^2 + Z^2(d)}{2\sigma^2}\right) I_0\left(\frac{Z(d) \times a}{\sigma^2}\right),$$

where $Z(d) \geq 0$, $a \geq 0$, and a is the envelope of the received signal, σ^2 is the deviation of the scattering signal power, Z is the amplitude of the dominant signal, which is based on propagation distance d , $I_0(\cdot)$ is the modified Bessel Function of the first kind and zero order. For the dominant signal, we can have

$$Z^2(d) = P_t \left(\frac{\lambda}{4\pi d}\right)^\alpha,$$

where $Z(d)$ is the peak amplitude of the dominant signal, P_t is the transmit power, α is the path loss exponent, λ is the wavelength of the signal, and d is the propagation distance. The Rician distribution is often described in terms of a

parameter K , known as the Rician factor, and is expressed as:

$$K(d) = 10 \log_{10} \frac{Z^2(d)}{2\sigma^2} \text{ dB.}$$

So we can have the expectation of H :

$$\mathbb{E}[H] = \frac{\mathbb{E}[A^2]}{2} = \text{Var}_a + (\mathbb{E}[A])^2,$$

where $\text{Var}_a = 2\sigma^2 + Z^2(d) - \frac{\pi\sigma^2}{2} L_{\frac{1}{2}}^2\left(\frac{-Z^2(d)}{2\sigma^2}\right)$ is the variance of A , $\mathbb{E}[A] = \sigma\sqrt{\frac{\pi}{2}} L_{\frac{1}{2}}\left(\frac{-Z^2(d)}{2\sigma^2}\right)$, and $L_a(x)$ denotes a *Laguerre polynomial* of degree a for input x .

3) *Channel Model Between SAT and SSs*: Shadowed-Rician (SR) channel model [37] is applied widely in literature in the communication link between SAT and SS. The received signal power can be written as follows.

$$P_r = P_t \left(\frac{\lambda}{4\pi d}\right)^{\alpha_{\text{sat}}} g_t g_r s w_r, \quad (6)$$

where P_t is the transmit power, λ is the wavelength of the carrier signal, α_{sat} is the path loss exponent, d is the distance between the transmitter and the receiver, g_t , g_r and s are the transmitter antenna gain, receiver antenna gain and the average rain attenuation, w_r is the SR fading in power which has a cumulative distribution function (CDF) shown as follows.

$$F_{w_r}(w) = \left(\frac{2b_0 m}{2b_0 m + \Omega}\right)^m \sum_{z=0}^{\infty} \binom{m}{z} \frac{\Omega}{z! \Gamma(z+1)} \left(\frac{\Omega}{2b_0 m + \Omega}\right)^z \times \gamma\left(z+1, \frac{1}{2b_0} w\right),$$

where $\Gamma(\cdot)$ denotes the *Gamma function*, $\gamma(\cdot, \cdot)$ is the *Lower incomplete gamma function*, $\binom{m}{z}$ is the *Pochhammer symbol*, and m, b_0, Ω are the factors of the SR fading.

C. Association Policy and CP

To make full use of the SAGSIN and achieve the best CP, SS will connect to the strongest relay among the nearest relay of four different tiers (OSs, TBs, HAPs, and SATs). Hence, the CP can be written as:

$$\begin{aligned} & \mathbb{P}_{\text{cov}}(\text{SINR} > \tau) \\ &= A_{\text{os}} \mathbb{P}(\text{SINR}_{\text{os}} > \tau) + A_{\text{tb}} \mathbb{P}(\text{SINR}_{\text{tb}} > \tau) \\ & \quad + A_{\text{hap}} \mathbb{P}(\text{SINR}_{\text{hap}} > \tau) + A_{\text{sat}} \mathbb{P}(\text{SINR}_{\text{sat}} > \tau) \\ &= A_{\text{os}}(D_{\text{os}}) \mathbb{P}\left(\frac{P_{r,\text{os}}(D_{\text{os}})}{I_{\text{os}} + \sigma_n^2} > \tau\right) + A_{\text{tb}}(D_{\text{tb}}) \mathbb{P}\left(\frac{P_{r,\text{tb}}(D_{\text{tb}})}{I_{\text{tb}} + \sigma_n^2} > \tau\right) \\ & \quad + A_{\text{hap}}(D_{\text{hap}}) \mathbb{P}\left(\frac{P_{r,\text{hap}}(D_{\text{hap}})}{I_{\text{hap}} + \sigma_n^2} > \tau\right) \\ & \quad + A_{\text{sat}}(D_{\text{sat}}) \mathbb{P}\left(\frac{P_{r,\text{sat}}(D_{\text{sat}})}{\sigma_n^2} > \tau\right), \end{aligned} \quad (7)$$

where $A_i(D_i)$, $i \in \{\text{os}, \text{tb}, \text{hap}, \text{sat}\}$ means the probability that the nearest relay station of the tier i is the strongest, and it is based on the nearest distance in each tier D_i . SINR_i , $i \in \{\text{os}, \text{tb}, \text{hap}, \text{sat}\}$ are the signal-to-interference-plus-noise ratio (SINR) of the nearest relay station of the tier i . $P_{r,i}(D_i)$, $i \in \{\text{os}, \text{tb}, \text{hap}, \text{sat}\}$ is the desired received signal power at the SS from its associated relay at tier i which is based on

the nearest distance in the tier, D_i . σ_n^2 and τ are the noise power and the decoding threshold, which are assumed to be known. Regarding the SAT, there is no interference since each SS will be covered by one SAT. I_j , $j \in \{\text{os}, \text{tb}, \text{hap}\}$ is the interference of the nearest relay station in the tier of j . Regarding the interference in each tier, the second nearest relay station in each tier will be considered as the main source of interference, and the second nearest distance, $D_{j,2}$, $j \in \{\text{os}, \text{tb}, \text{hap}\}$, will be taken into calculation exactly. Regarding the interference, except for the second nearest relay station, such as the third, fourth, and fifth nearest relay stations, etc., the influence of them will be calculated approximately, and the expectation of it can be derived into a function based on the second nearest distance $D_{j,2}$. Hence, the interference in each tier can be derived into a function based on the second nearest distance in each tier. So, we can have the CP as follows.

$$\begin{aligned} & \mathbb{P}_{\text{cov}}(\text{SINR} > \tau) \\ &= A_{\text{os}}(D_{\text{os}}) \mathbb{P}\left(\frac{P_{r,\text{os}}(D_{\text{os}})}{I_{\text{os}}(D_{\text{os},2}) + \sigma_n^2} > \tau\right) \\ & \quad + A_{\text{tb}}(D_{\text{tb}}) \mathbb{P}\left(\frac{P_{r,\text{tb}}(D_{\text{tb}})}{I_{\text{tb}}(D_{\text{tb},2}) + \sigma_n^2} > \tau\right) \\ & \quad + A_{\text{hap}}(D_{\text{hap}}) \mathbb{P}\left(\frac{P_{r,\text{hap}}(D_{\text{hap}})}{I_{\text{hap}}(D_{\text{hap},2}) + \sigma_n^2} > \tau\right) \\ & \quad + A_{\text{sat}}(D_{\text{sat}}) \mathbb{P}\left(\frac{P_{r,\text{sat}}(D_{\text{sat}})}{\sigma_n^2} > \tau\right). \end{aligned} \quad (8)$$

III. DISTRIBUTIONS OF DISTANCES BETWEEN SS AND THE FOUR TYPES OF RELAYS

In order to calculate the received signal power and signal-to-interference-plus-noise ratio (SINR) of the four different types of relays, it is necessary to compute the propagation distance distribution between each type of relay station and SS. Since SS will connect to the strongest relay among the nearest of each tier, the nearest distance between SS and OS or TB, or HAP is modeled as follows.

$$\begin{cases} D_{\text{os}} = \sqrt{(X_{\text{ss}} - X_{\text{os}})^2 + Y_{\text{os}}^2 + (h_{\text{os}} - h_{\text{ss}})^2} \\ D_{\text{tb}} = \sqrt{(X_{\text{ss}} - X_{\text{tb}})^2 + Y_{\text{tb}}^2 + (h_{\text{tb}} - h_{\text{ss}})^2} \\ D_{\text{hap}} = \sqrt{(X_{\text{ss}} - X_{\text{hap}})^2 + Y_{\text{hap}}^2 + (h_{\text{hap}} - h_{\text{ss}})^2}, \end{cases} \quad (9)$$

where X_{os} , and X_{tb} are 0 (over the coastline), X_{hap} can be set as required or optimized to achieve a better coverage performance, h_{os} , h_{tb} , h_{hap} , and h_{ss} are known, X_{ss} is given, Y_{os} , Y_{tb} , Y_{hap} are the distances from the projection of the SS on the y-axis to the nearest OS, TB, and HAP, all of those are modeled as 1D-PPP with densities of γ_{os} , γ_{tb} , and γ_{hap} . The distribution of the nearest distance between each type of relay station and SSs is calculated as follows. OS, TB, and HAP will be discussed first, and SAT will be discussed afterward.

Lemma 1: The PDFs of the nearest distance and the n -th nearest distance in 1D-PPP with the density of γ are given by [39]

$$f_{D_1}(d_1) = \gamma e^{-\gamma d_1}, \quad (10)$$

$$f_{D_n}(d_n) = \frac{\gamma^n d_n^{n-1}}{(n-1)!} e^{-\gamma d_n}. \quad (11)$$

Then the PDFs of D_{os} , D_{tb} , and D_{hap} are given by

$$f_{D_{os}}(d_{os}) = \frac{\gamma_{os} d_{os} \exp\left(-\gamma_{os} \sqrt{d_{os}^2 - (X_{ss} - X_{os})^2 - (h_{os} - h_{ss})^2}\right)}{\left(d_{os}^2 - (X_{ss} - X_{os})^2 - (h_{os} - h_{ss})^2\right)^{\frac{1}{2}}}, \quad (12)$$

where $d_{os} \geq \sqrt{(X_{ss} - X_{os})^2 + (h_{os} - h_{ss})^2}$.

$$f_{D_{tb}}(D_{tb}) = \frac{\gamma_{tb} D_{tb} \exp\left(-\gamma_{tb} \sqrt{D_{tb}^2 - (X_{ss} - X_{tb})^2 - (h_{tb} - h_{ss})^2}\right)}{\left(D_{tb}^2 - X_{ss}^2 - (h_{tb} - h_{ss})^2\right)^{\frac{1}{2}}}, \quad (13)$$

where $D_{tb} \geq \sqrt{(X_{ss} - X_{tb})^2 + (h_{tb} - h_{ss})^2}$. $f_{D_{hap}}(D_{hap})$ is shown in (14) at the bottom of the next page where $D_{hap} \geq \sqrt{(X_{ss} - X_{hap})^2 + (h_{os} - h_{ss})^2}$.

Proof: See Appendix A. \square

Besides the nearest distances, D_{os} , D_{tb} , and D_{hap} , we will calculate the exact value of the second nearest distances, which will be regarded as the primary source of interference and the approximation of the other interference will also be considered later. As we have $D_{os} = \sqrt{(X_{ss} - X_{os})^2 + Y_{os}^2 + (h_{os} - h_{ss})^2}$, where Y_{os} is the nearest distance in 1D-PPP, we can also have $D_{os,i} = \sqrt{(X_{ss} - X_{os})^2 + Y_{os,i}^2 + (h_{os} - h_{ss})^2}$, $i = 2, 3, 4, \dots$, which is the i -th nearest distance related to the i -th nearest interfering relay station, and $Y_{os,i}$ is the i -th nearest distance in 1D-PPP. Based on $f_{Y_{os}}(y_{os}) = \gamma_{os} e^{-\gamma_{os} y_{os}}$, we can calculate the PDF of $Y_{os,2}$ and $D_{os,2}$ in the following Lemma.

Lemma 2: The distribution of $Y_{os,2}$ conditioned on Y_{os} is given by [40]

$$f(y_{os,2}|y_{os}) = \gamma_{os} \exp\left(-\gamma_{os}(y_{os,2} - y_{os})\right). \quad (15)$$

So, the CDF of $D_{os,2}$ conditioned on y_{os} is

$$F_{D_{os,2}}(d_{os,2}|y_{os}) = 1 - \exp\left(-\gamma_{os} \left(\sqrt{d_{os,2}^2 - (X_{ss} - X_{os})^2 - (h_{os} - h_{ss})^2} - y_{os}\right)\right). \quad (16)$$

Proof: See Appendix B. \square

Based on the cumulative distribution function (CDF) of the second nearest distance conditioned on the nearest distance in (16) and $D_{os} = \sqrt{(X_{ss} - X_{os})^2 + Y_{os}^2 + (h_{os} - h_{ss})^2}$, we can get the PDF of the second nearest distance conditioned on the nearest distance as shown in (17) (at the bottom of the next page). The derivation of PDFs of the second nearest distance conditioned on the nearest distance between SS and TB or HAP is very similar to OS. For simplicity, we give the final expressions in (18) and (19) (at the bottom of the next page), where γ_{tb} and γ_{hap} are the densities of TB and HAP. The distribution of the distance to the second nearest relay station in each tier is important for the analysis of SINR since it represents the nearest interferer, which will be critical in our proposed dominant-interferer approximation.

The SAT is different from the other three types of relay stations since one SS will connect to only one SAT at one time.

Due to the high cost of satellite communication, the position of each satellite is calculated, especially for Low Earth Orbit satellites. Therefore, avoiding duplication of coverage to users (without interference) is one of the important tasks of satellite design [37], [41], [42]. Hence, there is no interference during satellite-based communication in this paper. We assume that a given number of SATs are evenly distributed in the low Earth orbit (LEO) at a given height h_{sat} . The distance between the SAT and the SS on the sea surface can be shown in Fig. 3, and the distribution of the distance between SAT and SS can be calculated as follows.

Lemma 3: Assuming n_{sat} satellites uniformly distributed over a spherical surface with radius r_d con-centric with the earth, the CDF of D_{sat} is [43]

$$F_{D_{sat}}(d_{sat}) = 1 - \mathbb{P}(D_{sat} > d_{sat}) = \begin{cases} 0, & d_{sat} < h_{sat} \\ 1 - \left(1 - \frac{1}{\pi} \arccos\left(1 - \frac{d_{sat}^2 - h_{sat}^2}{2r_d r_d}\right)\right)^{n_{sat}}, & h_{sat} \leq d_{sat} \leq d_{sat}^{\max} \\ 1 - \left(1 - \frac{1}{\pi} \arccos\left(\frac{r_e}{r_d}\right)\right)^{n_{sat}}, & d_{sat} > d_{sat}^{\max}, \end{cases} \quad (20)$$

where n_{sat} is the number of SAT, $r_d = h_{sat} + r_e$ is the distance between the center of Earth and the LEO satellite, r_e is the Earth radius, h_{sat} is the height of LEO satellite over the Earth surface, $z_d = r_d - h_d$ is the height of the Spherical Cap (which is shown in Fig. 3), $h_d = \frac{D_{sat}^2 - h_{sat}^2}{2r_e}$ is the thickness of the Spherical Cap, $d_{sat}^{\max} = \sqrt{h_{sat}^2 + 2h_{sat}r_e}$.

Proof: See Appendix C. \square

Besides the distributions of the distance between the four different types of relay stations and SSs, constraints on communication distance between the relay station and SS must be considered. Due to the fact that the Earth is a sphere rather than a plane, any connection via a straight-line propagation path is limited by the distance between the transmitter and the receiver. As shown in Fig. 4, due to the Earth being a sphere instead of a plane, space/air-sea surface communication can not get through the earth. Therefore, there must be a maximum propagation distance in the space/air-to-sea surface link, and it depends on the transmitter's and receiver's heights. Derived from the geometry, we can calculate the maximum line-of-sight communication distance between two objects in the air and on the Earth's surface as follows.

$$\begin{cases} \frac{\sin(\beta)}{r_e + h_y} = \frac{\sin(90^\circ + \phi)}{r_e + h_x} \\ \beta = \arcsin\left(\frac{(r_e + h_y) \sin(90^\circ + \phi)}{r_e + h_x}\right) \\ d = \frac{(r_e + h_y) \sin(90^\circ - \phi - \beta)}{\sin(\beta)} \end{cases}, \quad (21)$$

where r_e is the radius of the Earth, d is the propagation distance, h_x and h_y are two heights of the relay station, and SS, ϕ is the pitch angle of the arrived signal at the end-user on the ground. Based on (21), when $\phi = 0^\circ$, the transmitted signal from the aerial station will be a tangent to the earth (a sphere). At this time, the distance between the end-user and the aerial station is the longest distance, and d^{\max} is indicated as the maximum propagation distance. Hence, the maximum line-of-sight communication distance between two objects in the air and on the Earth's surface is clarified in Lemma 4.

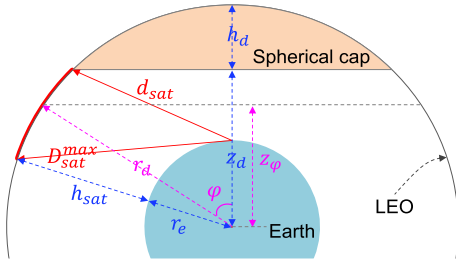


Fig. 3. Distance between SS and SAT.

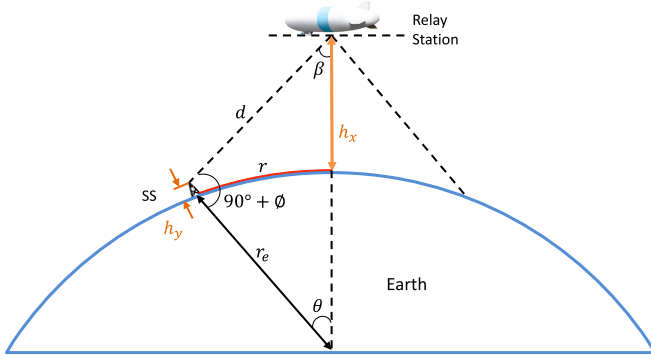


Fig. 4. Maximum propagation distance between end user and relay station.

Lemma 4: The maximum propagation distance between the SS and OS, TB, HAP, or SAT can be given by

$$\begin{cases} d_{os}^{\max} &= \sqrt{(r_e + h_{os})^2 - (r_e + h_{ss})^2} \\ d_{tb}^{\max} &= \sqrt{(r_e + h_{tb})^2 - (r_e + h_{ss})^2} \\ d_{hap}^{\max} &= \sqrt{(r_e + h_{hap})^2 - (r_e + h_{ss})^2} \\ d_{sat}^{\max} &= \sqrt{(r_e + h_{sat})^2 - (r_e + h_{ss})^2} \end{cases} \quad (22)$$

where h_{ss} , h_{os} , h_{hap} , h_{sat} denote heights of SS, OS, TB, HAP, and SAT.

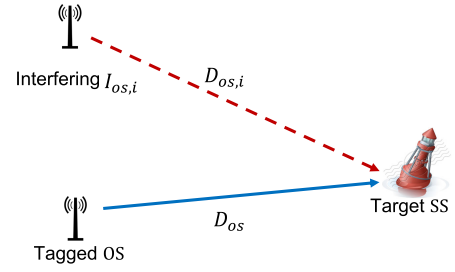


Fig. 5. Coverage model between SS and OS.

IV. MATHEMATICAL ANALYSIS OF THE CP

In this section, we will provide the mathematical analysis of the CP of the SAGSIN and get the final expression of the CP. An example of the nearest distance and interfering distance is shown in Fig. 5. Assuming that the tagged relay station is an OS, the nearest distance between the tagged OS and the target SS is noted as D_{os} , and other OSs are regarded as interference with interfering distances $D_{os,i}$. So we can model the interfering distances $D_{os,i}$ and interfering OSs, $I_{os,i}$, as $\{D_{os,i} | I_{os,i} \in \Phi_{os}, i = 2, 3, 4, \dots\}$, where Φ_{os} is the set of the interfering OSs. Similarly, we can have the model of interference in each tier as $\{D_{j,i} | I_{j,i} \in \Phi_j, j = \{os, tb, hap, sat\}, i = 2, 3, 4, \dots\}$. Since the SS connects with the nearest relay station, D_j is always less than $D_{j,i}$, $j = \{os, tb, hap, sat\}, i = 2, 3, 4, \dots$. Besides that, according to (22), the maximum propagation distances between SS and each relay station are marked as d_{os}^{\max} , d_{tb}^{\max} , d_{hap}^{\max} , d_{sat}^{\max} , and the propagation distances of both the desired signal and the interference signal are less than the maximum. During the communication of SAT and SS, there is no interference, which means that at one time, each SS can only be covered by one SAT, which is the tagged SAT.

In order to calculate the CP of the SAGSIN, we need to compute the desired signal power, which is related to the nearest distance in each tier, and then the strongest relay will

$$f_{D_{hap}}(D_{hap}) = \frac{\gamma_{hap} D_{hap} \exp(-\gamma_{hap} \sqrt{D_{hap}^2 - (X_{ss} - X_{hap})^2 - (h_{hap} - h_{ss})^2})}{(D_{hap}^2 - (X_{ss} - X_{hap})^2 - (h_{hap} - h_{ss})^2)^{\frac{1}{2}}}, \quad (14)$$

$$f_{D_{os,2}}(d_{os,2} | d_{os}) = \frac{\gamma_{os} \exp\left(-\gamma_{os} \left(\sqrt{d_{os,2}^2 - (X_{ss} - X_{os})^2 - (h_{os} - h_{ss})^2} - \sqrt{d_{os}^2 - (X_{ss} - X_{os})^2 - (h_{os} - h_{ss})^2}\right)\right)}{d_{os,2}^{-1} \sqrt{d_{os,2}^2 - (X_{ss} - X_{os})^2 - (h_{os} - h_{ss})^2}}. \quad (17)$$

$$f_{D_{tb,2}}(d_{tb,2} | d_{tb}) = \frac{\gamma_{tb} \exp\left(-\gamma_{tb} \left(\sqrt{d_{tb,2}^2 - (X_{ss} - X_{tb})^2 - (h_{tb} - h_{ss})^2} - \sqrt{d_{tb}^2 - (X_{ss} - X_{tb})^2 - (h_{tb} - h_{ss})^2}\right)\right)}{d_{tb,2}^{-1} \sqrt{d_{tb,2}^2 - (X_{ss} - X_{tb})^2 - (h_{tb} - h_{ss})^2}}. \quad (18)$$

$$f_{D_{hap,2}}(d_{hap,2} | d_{hap}) = \frac{\gamma_{hap} \exp\left(-\gamma_{hap} \left(\sqrt{d_{hap,2}^2 - (X_{ss} - X_{hap})^2 - (h_{hap} - h_{ss})^2} - \sqrt{d_{hap}^2 - (X_{ss} - X_{hap})^2 - (h_{hap} - h_{ss})^2}\right)\right)}{d_{hap,2}^{-1} \sqrt{d_{hap,2}^2 - (X_{ss} - X_{hap})^2 - (h_{hap} - h_{ss})^2}}. \quad (19)$$

be chosen as the tagged relay. The association probability of each tier will be calculated according to the association policy. Finally, the total CP will be derived.

A. Desired Received Signal Power at SS From Each Type of Relay Station

In a SAGSIN, a comparison of desired received power from each type of relay station should be executed to decide which kind of relay station will be selected as the tagged station. Desired signal power comes from different relay stations with different channels, which are shown in section II and can be written as follows.

1) Desired Signal Power From OS to SS:

$$\begin{aligned} P_{r,os}(D_{os}) &= P_{t,os} 10^{0.1L_{ITU}(D_{os})} g_t^{os} g_r^{ss} \\ &= P_{t,os} 10^{0.1(-139.3+E(D_{os})-20\log(f_{os}/10^6))} g_t^{os} g_r^{ss} \\ &\triangleq C_{r,os} \mathcal{A}(D_{os}), \end{aligned} \quad (23)$$

where $L_{ITU}(D_{os})$ and $E(D_{os})$ are shown in (3), f_{os} is the frequency, $\mathcal{A}(D_{os}) = 10^{0.1E(D_{os})}$ is a function based on D_{os} , and $C_{r,os} = P_{t,os} \times 10^{0.1(-139.3-20\log(f_{os}/10^6))} g_t^{os} g_r^{ss}$ is a constant.

2) Desired Signal Power From TB to SS:

$$P_{r,tb}(D_{tb}) \triangleq C_{r,tb} \mathcal{B}(D_{tb}), \quad (24)$$

where $C_{r,tb} = g_t^{tb} g_r^{ss}$ is a constant, $\mathcal{B}(D_{tb}) = H_{r,tb}(D_{tb})$, and we have

$$\begin{aligned} \mathbb{E}[H_{r,tb}(D_{tb})] &= 2\sigma_{tb}^2 + Z_{tb}^2(D_{tb}) - \frac{\pi\sigma_{tb}^2}{2} L_{\frac{1}{2}}^2\left(\frac{-Z_{tb}^2(D_{tb})}{2\sigma_{tb}^2}\right) \\ &\quad + \left(\sigma_{tb} \sqrt{\frac{\pi}{2}} L_{\frac{1}{2}}\left(\frac{-Z_{tb}^2(D_{tb})}{2\sigma_{tb}^2}\right)\right)^2, \end{aligned}$$

where $10\log_{10} \frac{Z_{tb}^2(D_{tb})}{2\sigma_{tb}^2} \triangleq K_{tb}$ which is given in dB and

$Z_{tb}^2(D_{tb}) = P_{t,tb} \left(\frac{\lambda_{tb}}{4\pi D_{tb}}\right)^{\alpha_{tb}}$, and λ_{tb} is the wavelength.

3) Desired Signal Power From HAP to SS:

$$P_{r,hap}(D_{hap}) \triangleq C_{r,hap} \mathcal{C}(D_{hap}), \quad (25)$$

where $C_{r,hap} = g_t^{hap} g_r^{ss}$ is a constant, $\mathcal{C}(D_{hap}) = H_{r,hap}(D_{hap})$, and we have

$$\begin{aligned} \mathbb{E}[H_{r,hap}(D_{hap})] &= 2\sigma_{hap}^2 + Z_{hap}^2(D_{hap}) \\ &\quad - \frac{\pi\sigma_{hap}^2}{2} L_{\frac{1}{2}}^2\left(\frac{-Z_{hap}^2(D_{hap})}{2\sigma_{hap}^2}\right) \\ &\quad + \left(\sigma_{hap} \sqrt{\frac{\pi}{2}} L_{\frac{1}{2}}\left(\frac{-Z_{hap}^2(D_{hap})}{2\sigma_{hap}^2}\right)\right)^2, \end{aligned}$$

where $10\log_{10} \frac{Z_{hap}^2(D_{hap})}{2\sigma_{hap}^2} \triangleq K_{hap}$ which is given in dB and $Z_{hap}^2(D_{hap}) = P_{t,hap} \left(\frac{\lambda_{hap}}{4\pi D_{hap}}\right)^{\alpha_{hap}}$, and λ_{hap} is the wavelength.

4) Desired Signal Power From SAT to SS:

$$P_{r,sat}(D_{sat}) \triangleq C_{r,sat} \mathcal{D}(D_{sat}), \quad (26)$$

where $C_{r,sat} = P_{t,sat} \left(\frac{\lambda_{sat}}{4\pi}\right)^{\alpha_{sat}} g_t^{sat} g_r^{ss} s w_r$ is a constant, λ_{sat} is the wavelength, $\mathcal{D}(D_{sat}) = \frac{1}{D_{sat}^{\alpha_{sat}}}$, and we have

$$\begin{aligned} F_{w_r}(w) &= \left(\frac{2b_0 m}{2b_0 m + \Omega}\right)^m \sum_{z=0}^{\infty} \left(\frac{(m)_z}{z! \Gamma(z+1)}\right. \\ &\quad \left. \times \left(\frac{\Omega}{2b_0 m + \Omega}\right)^z \gamma(z+1, \frac{1}{2b_0} w)\right), \end{aligned}$$

where $\Gamma(\cdot)$ denotes the Gamma function, $\gamma(\cdot, \cdot)$ is the Lower incomplete gamma function, $(m)_z$ is the Pochhammer symbol, and m, b_0, Ω are the factors of the SR fading.

B. Association Probability of Each Tier of Relay Station

In cooperative SAGSINs with four different types of relay stations, the association probability of each type of relay station means the probability that the SS at a given distance from the coastline will associate with this type of relay station. The association probability is decided by the desired received signal power from each type of relay. The total CP equals the summation of the associated probability of each tier times the CP of each tier, and with the given distance between SS and coastline, X_{ss} , it can be written as:

$$\begin{aligned} \mathbb{P}_{cov}(\text{SINR} > \tau) &= \mathbb{E}_{D_{os,2}} \mathbb{E}_{D_{os}} \left[A_{os}(D_{os}) \mathbb{P}(\text{SINR}_{os} > \tau | D_{os}, D_{os,2}) \right] \\ &\quad + \mathbb{E}_{D_{tb,2}} \mathbb{E}_{D_{tb}} \left[A_{tb}(D_{tb}) \mathbb{P}(\text{SINR}_{tb} > \tau | D_{tb}, D_{tb,2}) \right] \\ &\quad + \mathbb{E}_{D_{hap,2}} \mathbb{E}_{D_{hap}} \left[A_{hap}(D_{hap}) \mathbb{P}(\text{SINR}_{hap} > \tau | D_{hap}, D_{hap,2}) \right] \\ &\quad + \mathbb{E}_{D_{sat}} \left[A_{sat}(D_{sat}) \mathbb{P}(\text{SINR}_{sat} > \tau | D_{sat}) \right], \end{aligned} \quad (27)$$

where $A_{os}(D_{os})$, $A_{tb}(D_{tb})$, $A_{hap}(D_{hap})$, $A_{sat}(D_{sat})$ are four association probabilities, $\mathbb{P}_{os}(\text{SINR}_{os} > \tau | D_{os}, D_{os,2})$, $\mathbb{P}_{tb}(\text{SINR}_{tb} > \tau | D_{tb}, D_{tb,2})$, $\mathbb{P}_{hap}(\text{SINR}_{hap} > \tau | D_{hap}, D_{hap,2})$, $\mathbb{P}_{sat}(\text{SINR}_{sat} > \tau | D_{sat})$ are four CP in each relay station tier, τ is the given threshold of the received SINR to enable signal decoding.

Theorem 1: Association probability is the probability that a particular type of relay will be selected as the tagged relay. The association probability of OS is calculated as follows.

$$\begin{aligned} A_{os}(D_{os}) &= \int_{d'_{tb}}^{\infty} \left(\mathbb{1}(d_{tb} \leq d_{tb}^{\max}) \mathbb{1}(\mathcal{B}(d_{tb}) < \frac{C_{r,os}}{C_{r,tb}} \mathcal{A}(D_{os})) \right. \\ &\quad \left. + \mathbb{1}(d_{tb} > d_{tb}^{\max}) \right) f_{D_{tb}}(d_{tb}) dd_{tb} \\ &\quad \times \int_{d'_{hap}}^{\infty} \left(\mathbb{1}(d_{hap} \leq d_{hap}^{\max}) \mathbb{1}(\mathcal{C}(d_{hap}) < \frac{C_{r,os}}{C_{r,hap}} \mathcal{A}(D_{os})) \right. \\ &\quad \left. + \mathbb{1}(d_{hap} > d_{hap}^{\max}) \right) f_{D_{hap}}(d_{hap}) dd_{hap} \\ &\quad \times \left(1 - F_{D_{sat}} \left(\mathcal{D}^{-1} \left(\frac{C_{r,os}}{C_{r,sat}} \mathcal{A}(D_{os}) \right) \right) \right), \end{aligned} \quad (28)$$

where

$$\begin{cases} d'_{os} = \sqrt{(X_{ss} - X_{os})^2 + (h_{ss} - h_{os})^2} \\ d'_{tb} = \sqrt{(X_{ss} - X_{tb})^2 + (h_{ss} - h_{tb})^2} \\ d'_{hap} = \sqrt{(X_{ss} - X_{hap})^2 + (h_{ss} - h_{hap})^2} \end{cases}, \quad (29)$$

and we can find that the association probability of OS is based on the nearest distance between the SS and the OS, D_{os} . *Proof:* See Appendix D. \square

Remark 1: In (28), we can find the association policy clearly, which is the comparison of the four strongest received signals in the four tiers. We can also notice that the association probability is a combination of the comparison of received signal power and the comparison between the parameter X_{ss} and the related maximum coverage range. Besides that, we can find the CP of the four different relay stations, $\mathbb{P}(\text{SINR}_i \geq \tau)$, $i \in \{OS, TB, HAP, SAT\}$, is not involved. Hence, the situation that the association probability of one particular tier is not zero, but that the CP of the tier is zero may happen, or the opposite may happen, which means that sometimes, the SS may not be covered by the SAGSIN, and the summation of CPs of the four different relay stations does not equal to 1.

The derivation approach of association probabilities of TB, HAP, and SAT are similar to OS's, so we provide the calculation process of A_{os} in the appendix in detail and list the final expressions of $A_{tb}(D_{tb})$, $A_{hap}(D_{hap})$, $A_{sat}(D_{sat})$ while the proof is omitted.

$$\begin{aligned} A_{tb}(D_{tb}) &= \int_{d'_{os}}^{\infty} \left(\mathbb{1}(d_{os} \leq d_{os}^{\max}) \mathbb{1}(\mathcal{A}(d_{os}) < \frac{C_{r,tb}}{C_{r,os}} \mathcal{B}(D_{tb})) \right. \\ &\quad \left. + \mathbb{1}(d_{os} > d_{os}^{\max}) \right) f_{D_{os}}(d_{os}) dd_{os} \\ &\quad \times \int_{d'_{hap}}^{\infty} \left(\mathbb{1}(d_{hap} \leq d_{hap}^{\max}) \mathbb{1}(\mathcal{C}(d_{hap}) < \frac{C_{r,tb}}{C_{r,hap}} \mathcal{B}(D_{tb})) \right. \\ &\quad \left. + \mathbb{1}(d_{hap} > d_{hap}^{\max}) \right) f_{D_{hap}}(d_{hap}) dd_{hap} \\ &\quad \times \left(1 - F_{D_{sat}} \left(\mathcal{D}^{-1} \left(\frac{C_{r,tb}}{C_{r,sat}} \mathcal{B}(D_{tb}) \right) \right) \right), \end{aligned} \quad (30)$$

$$\begin{aligned} A_{hap}(D_{hap}) &= \int_{d'_{os}}^{\infty} \left(\mathbb{1}(d_{os} \leq d_{os}^{\max}) \mathbb{1}(\mathcal{A}(d_{os}) < \frac{C_{r,hap}}{C_{r,os}} \mathcal{C}(D_{hap})) \right. \\ &\quad \left. + \mathbb{1}(d_{os} > d_{os}^{\max}) \right) f_{D_{os}}(d_{os}) dd_{os} \\ &\quad \times \int_{d'_{tb}}^{\infty} \left(\mathbb{1}(d_{tb} \leq d_{tb}^{\max}) \mathbb{1}(\mathcal{B}(d_{tb}) < \frac{C_{r,hap}}{C_{r,tb}} \mathcal{C}(D_{hap})) \right. \\ &\quad \left. + \mathbb{1}(d_{tb} > d_{tb}^{\max}) \right) f_{D_{tb}}(d_{tb}) dd_{tb} \\ &\quad \times \left(1 - F_{D_{sat}} \left(\mathcal{D}^{-1} \left(\frac{C_{r,hap}}{C_{r,sat}} \mathcal{C}(D_{hap}) \right) \right) \right), \end{aligned} \quad (31)$$

$$A_{sat}(D_{sat}) = \int_{d'_{os}}^{\infty} \left(\mathbb{1}(d_{os} \leq d_{os}^{\max}) \mathbb{1}(\mathcal{A}(d_{os}) < \frac{C_{r,sat}}{C_{r,os}} \mathcal{D}(D_{sat})) \right.$$

$$\begin{aligned} &\quad \left. + \mathbb{1}(d_{os} > d_{os}^{\max}) \right) f_{D_{os}}(d_{os}) dd_{os} \\ &\quad \times \int_{d'_{tb}}^{\infty} \left(\mathbb{1}(d_{tb} \leq d_{tb}^{\max}) \mathbb{1}(\mathcal{B}(d_{tb}) < \frac{C_{r,sat}}{C_{r,tb}} \mathcal{D}(D_{sat})) \right. \\ &\quad \left. + \mathbb{1}(d_{tb} > d_{tb}^{\max}) \right) f_{D_{tb}}(d_{tb}) dd_{tb} \\ &\quad \times \int_{d'_{hap}}^{\infty} \left(\mathbb{1}(d_{hap} \leq d_{hap}^{\max}) \mathbb{1}(\mathcal{C}(d_{hap}) < \frac{C_{r,sat}}{C_{r,hap}} \mathcal{D}(D_{sat})) \right. \\ &\quad \left. + \mathbb{1}(d_{hap} > d_{hap}^{\max}) \right) f_{D_{hap}}(d_{hap}) dd_{hap}, \end{aligned} \quad (32)$$

where $C_{r,os}$, $C_{r,tb}$, $C_{r,hap}$, $C_{r,sat}$, $\mathcal{A}(d_{os})$, $\mathcal{B}(d_{tb})$, $\mathcal{C}(d_{hap})$, $\mathcal{D}(d_{sat})$ can be found in (23), (24), (25), (26), PDF of D_{os} , D_{tb} , D_{hap} , D_{sat} are shown in Lemma 1 and Lemma 3, d_{os}^{\max} , d_{tb}^{\max} , d_{hap}^{\max} , d_{sat}^{\max} are maximum communication distances of OS, TB, HAP, SAT which are shown in Lemma 4.

C. Interference at SS From Each Type of Relay Station

Considering each relay station in SAGSIN, SINR of OS, TB, and HAP are needed, as shown in (8). Here we will derive the interference, $I_{os}(D_{os,2})$, in the tier of OS, and the interference of TB and HAP can be calculated easily in the same way.

Since the second nearest relay station is the main source of interference, we will calculate the effect of the second nearest relay station exactly and take an expectation over the other interfering relay stations based on the second nearest distance. Hence, according to the channel model shown in (23), the approximation of the interference in the tier of OS can be written as:

$$\hat{I}_{os} = C_{r,os} \mathcal{A}(D_{os,2}) + \mathbb{E}[I_{os,3}], \quad (33)$$

where $D_{os,2} = \sqrt{(X_{ss} - X_{os})^2 + Y_{os,2}^2 + (h_{os} - h_{ss})^2}$ which is the second nearest distance between OSs and the SS, $\mathbb{E}[I_{os,3}]$ is the expectation of the interference made by the relay stations including the third nearest distance and further interfering stations. Based on Campbell's theorem [39], we can calculate the expectation of the interference made by the third nearest and further interfering relay stations as follows.

$$\begin{aligned} \mathbb{E}[I_{os,3}] &= \mathbb{E} \left[\sum_{I_{os,i} \in \Phi_{os}} C_{r,os} \mathcal{A}(D_{os,i}), i = 3, 4, \dots \right] \\ &= C_{r,os} \mathbb{E} \left[\sum_{I_{os,i} \in \Phi_{os}} \mathcal{A}(D_{os,i}), i = 3, 4, \dots \right] \\ &= C_{r,os} \gamma_{os} \int_{D_{os,2}}^{d_{os}^{\max}} \mathcal{A}(x) dx. \end{aligned} \quad (34)$$

So we can get the interference in the tier of OS as a function based on the second nearest distance $D_{os,2}$ and have

$$I_{os}(D_{os,2}) \triangleq \hat{I}_{os}. \quad (35)$$

Similar to OS, the expectation of the interference in the tiers of TB and HAP can be written as:

$$\begin{cases} I_{tb}(D_{tb,2}) \triangleq \hat{I}_{tb} \\ = C_{r,tb} \mathcal{B}(D_{tb,2}) + C_{r,tb} \gamma_{tb} \int_{D_{tb,2}}^{d_{tb}^{\max}} \mathcal{B}(x) dx \\ I_{hap}(D_{hap,2}) \triangleq \hat{I}_{hap} \\ = C_{r,hap} \mathcal{C}(D_{hap,2}) + C_{r,hap} \gamma_{hap} \int_{D_{hap,2}}^{d_{hap}^{\max}} \mathcal{C}(x) dx \end{cases}. \quad (36)$$

D. Coverage Probability

The formula of total CP in the SAGSIN is shown in (27). This subsection gives the final expression of CP in the SAGSIN. The CP of each type of relay in the SAGSIN can be obtained by association probability times CP of that relay on the specific relay station. Then the final expression can be achieved by summing the coverage of the four relay stations. Here, we can get the CP of OS in SAGSIN as follows.

$$\begin{aligned} & \mathbb{E}_{D_{os,2}} \mathbb{E}_{D_{os}} [A_{os}(D_{os}) \mathbb{P}(\text{SINR}_{os} > \tau | D_{os}, D_{os,2})] \\ &= \mathbb{E}_{D_{os,2}} \mathbb{E}_{D_{os}} [A_{os}(D_{os}) \mathbb{P}\left(\frac{P_{r,os}(D_{os})}{I_{os} + \sigma_n^2} > \tau | D_{os}, D_{os,2}\right)] \\ &= \mathbb{E}_{D_{os,2}} \mathbb{E}_{D_{os}} [A_{os}(D_{os}) \mathbb{P}(P_{r,os}(D_{os}) \\ &> \tau(I_{os} + \sigma_n^2) | D_{os}, D_{os,2})]. \end{aligned} \quad (37)$$

Since we have the expectation of the interference of OS in (35), we can have

$$\begin{aligned} & \mathbb{E}_{D_{os,2}} \mathbb{E}_{D_{os}} [A_{os}(D_{os}) \mathbb{P}(\text{SINR}_{os} > \tau | D_{os}, D_{os,2})] \\ &= \int_{\min(d'_{os}, d_{os}^{\max})}^{d_{os}^{\max}} \int_{d_{os}}^{d_{os}^{\max}} A_{os}(d_{os}) \Xi_{os}(d_{os,2} | d_{os}) \\ &\quad \times f_{D_{os,2}}(d_{os,2} | d_{os}) dd_{os,2} f_{D_{os}}(d_{os}) dd_{os}, \end{aligned} \quad (38)$$

where $d'_{os} = \sqrt{(X_{ss} - X_{os})^2 + (h_{ss} - h_{os})^2}$, $A_{os}(d_{os})$ is shown in (28), and

$$\begin{aligned} & \Xi_{os}(d_{os,2} | d_{os}) \\ &= \mathbb{1}\left(\mathcal{A}(d_{os}) > \tau(\mathcal{A}(d_{os,2}) + \gamma_{os} \int_{d_{os,2}}^{d_{os}^{\max}} \mathcal{A}(x) dx + \frac{\sigma_n^2}{C_{r,os}})\right). \end{aligned} \quad (39)$$

Proof: See Appendix E. \square

Based on the results of association probability, the total CPs in (27) is shown as follows. The detailed process of CP of OS is given, and the calculations of the other three tiers are similar to OS. The final expression of the total CP can be written as:

$$\begin{aligned} & \mathbb{P}_{cov}(\text{SINR} > \tau) \\ &= \int_{\min(d'_{os}, d_{os}^{\max})}^{d_{os}^{\max}} \int_{d_{os}}^{d_{os}^{\max}} A_{os}(d_{os}) \Xi_{os}(d_{os,2} | d_{os}) \\ &\quad \times f_{D_{os,2}}(d_{os,2} | d_{os}) dd_{os,2} f_{D_{os}}(d_{os}) dd_{os} \\ &+ \int_{\min(d'_{tb}, d_{tb}^{\max})}^{d_{tb}^{\max}} \int_{d_{tb}}^{d_{tb}^{\max}} A_{tb}(d_{tb}) \Xi_{tb}(d_{tb,2} | d_{tb}) \\ &\quad \times f_{D_{tb,2}}(d_{tb,2} | d_{tb}) dd_{tb,2} f_{D_{tb}}(d_{tb}) dd_{tb} \\ &+ \int_{\min(d'_{hap}, d_{hap}^{\max})}^{d_{hap}^{\max}} \int_{d_{hap}}^{d_{hap}^{\max}} A_{hap}(d_{hap}) \Xi_{hap}(d_{hap,2} | d_{hap}) \\ &\quad \times f_{D_{hap,2}}(d_{hap,2} | d_{hap}) dd_{hap,2} f_{D_{hap}}(d_{hap}) dd_{hap} \\ &+ \int_{\min(h_{sat}, d_{sat}^{\max})}^{d_{sat}^{\max}} A_{sat}(d_{sat}) \mathbb{1}(d_{sat} < \mathcal{D}^{-1}(\frac{\tau \sigma_n^2}{C_{r,sat}})) \\ &\quad \times f_{D_{sat}}(d_{sat}) dd_{sat}, \end{aligned} \quad (40)$$

where $A_{os}(d_{os})$, $A_{tb}(d_{tb})$, $A_{hap}(d_{hap})$, $A_{sat}(d_{sat})$ are shown in (28), (30), (31), (32), $\Xi_{os}(d_{os,2} | d_{os})$, $\Xi_{tb}(d_{tb,2} | d_{tb})$, $\Xi_{hap}(d_{hap,2} | d_{hap})$ are CPs of OS, TB, HAP of each tier with given their desired distance, d'_{os} , d'_{tb} , and d'_{hap} are shown in (29), h_{sat} is the height of the SAT, PDF of the nearest

distance in each tier is shown in Lemma 1, PDF of the second nearest distance conditioned on the nearest distance in each tier is shown in Lemma 2. We give the final expressions of three relay stations as follows, and since their derivation process is similar, we only give the specific calculation process of OS in Appendix E. The other two derivations can be obtained accordingly.

$$\begin{cases} \Xi_{os}(d_{os,2} | d_{os}) \\ = \mathbb{1}\left(\mathcal{A}(d_{os}) > \tau(\mathcal{A}(d_{os,2}) + \gamma_{os} \int_{d_{os,2}}^{d_{os}^{\max}} \mathcal{A}(x) dx + \frac{\sigma_n^2}{C_{r,os}})\right) \\ \Xi_{tb}(d_{tb,2} | d_{tb}) \\ = \mathbb{1}\left(\mathcal{B}(d_{tb}) > \tau(\mathcal{B}(d_{tb,2}) + \gamma_{tb} \int_{d_{tb,2}}^{d_{tb}^{\max}} \mathcal{B}(x) dx + \frac{\sigma_n^2}{C_{r,tb}})\right) \\ \Xi_{hap}(d_{hap,2} | d_{hap}) \\ = \mathbb{1}\left(\mathcal{C}(d_{hap}) > \tau(\mathcal{C}(d_{hap,2}) + \gamma_{hap} \int_{d_{hap,2}}^{d_{hap}^{\max}} \mathcal{C}(x) dx + \frac{\sigma_n^2}{C_{r,hap}})\right). \end{cases}$$

Remark 2: When the parameter of X_{ss} increases to some particular bounds, the four types of relays will be out of choice in turns. Regarding the lower integral limits d'_{os} related to OS, since $d'_{os} = \sqrt{(X_{ss} - X_{os})^2 + (h_{ss} - h_{os})^2}$, when X_{ss} is greater than $\sqrt{(d_{os}^{\max})^2 - (h_{ss} - h_{os})^2} + X_{os}$, d'_{os} will be greater than d_{os}^{\max} which indicate the performance of related relay station turns unfruitful. Similar situations should happen in the tier of TB and HAP. When X_{ss} is greater than $\sqrt{(d_{tb}^{\max})^2 - (h_{ss} - h_{os})^2} + X_{os}$ and $\sqrt{(d_{hap}^{\max})^2 - (h_{ss} - h_{os})^2} + X_{os}$, d'_{tb} and d'_{hap} will be greater than d_{tb}^{\max} and d_{hap}^{\max} which indicate the performance of related relay stations turns unfruitful.

V. NUMERICAL ANALYSIS AND SIMULATIONS

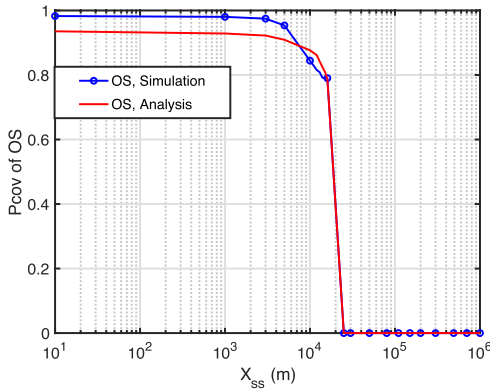
In this section, we will verify the accuracy of the derived expression for the CP in SAGSIN using the Monte Carlo simulation method. In addition, by comparing the coverage performance of SAGSIN with a single relay station, we will try to reveal some insights. The details of the simulation setup are shown in Table I.

A. Results of Analysis and Simulation

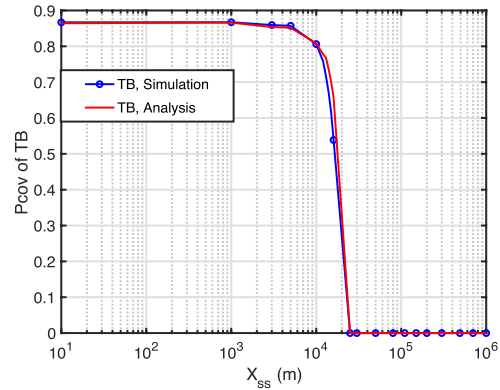
Firstly, in Fig. 6, the CPs to SS with a single type of relay station, including analysis and simulation results, are shown, where we can see that all the analysis results match with simulations well, it shows the credibility of the analysis. In Fig. 6(a), 6(b), 6(c), OS, TB, and HAP achieve good performance when the distance between SS and the coastline, X_{ss} is small. However, as X_{ss} increases, they cannot cover the SSs anymore, and the CPs drop to 0 quickly. Due to the earth being a sphere, the maximum X_{ss} that the OS can cover is limited to around 22 km. Similarly, TB and HAP also have maximum coverage distances, which are around 80 km and 500 km. When the distance between SS and the coastline is greater than the maximum coverage distances of the relays, the connections will be dropped. In this scenario, with the increase of X_{ss} , OS, TB, and HAP will take turns to gain the performance advantage and be selected as the tagged relay station.

TABLE I
PARAMETERS USED IN THE SIMULATION

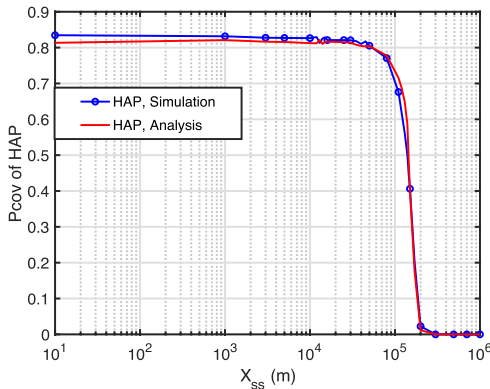
Notation	Parameter	Value
X_{os}, X_{tb}, X_{hap}	X coordinates of OS, TB, HAP	0, 0, 1000 (m)
$h_{os}, h_{tb}, h_{hap}, h_{sat}$	Heights of OS, TB, HAP, SAT	0.02, 0.5, 22, 550 (km)
h_{ss}	Height of SS	1 m
$\gamma_{os}, \gamma_{tb}, \gamma_{hap}$	Densities of OS, TB, HAP	$2 \times 10^{-4}, 10^{-4}, 10^{-5}$
n_{sat}	Number of SAT at LEO	100
$\alpha_{tb}, \alpha_{hap}, \alpha_{sat}$	Path loss exponent	2.7, 2.3, 2.3
s	The average rain attenuation	2 dB ^[38]
$f_{os}, f_{tb}, f_{hap}, f_{sat}$	Frequency	2.4 ^[7] , 1.5 ^[45] , 2 ^[46] , 20 ^[38] (GHz)
$P_{t,os}, P_{t,tb}, P_{t,hap}, P_{t,sat}$	Transmit power	30, 45, 45, 60 (dBm)
$G_t^{os}, G_t^{tb}, G_t^{hap}, G_t^{sat}$	Transmit antenna gain	30, 30, 41, 41 (dB)
G_r	Received antenna gain	10 dB
τ	Decoding threshold	-5 dB



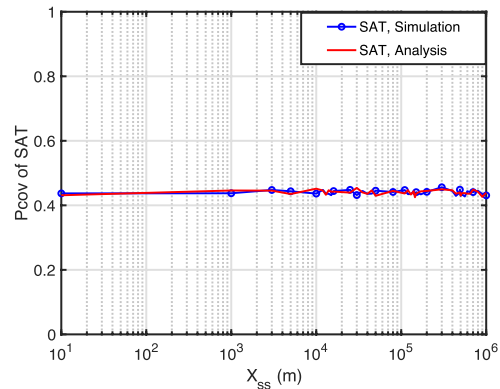
(a) Only relay on OS



(b) Only relay on TB



(c) Only relay on HAP



(d) Only relay on SAT

Fig. 6. CP of a single type of relay station.

In Fig. 6(d), we can see that SAT can cover a big range of X_{ss} , which is the biggest advantage of SAT-based communication. However, the CP performance is not very good, which remains at the level of 0.42. Comparing the four different types of relay stations' coverage performance, from OS to TB, HAP, and SAT, in the duration of their accessible range of X_{ss} , the obtainable best CPs for the four types of relays decrease (1, 0.85, 0.8, 0.42). Besides that, regarding the maximum X_{ss}

(the first place that the CP equals 0) that each type of relay station can cover, the four maximum X_{ss} related to OS, TB, HAP, and SAT increase. It shows that with a small range of X_{ss} where more than one type of relay is available, we can have different choices in different situations instead of relying on a single relay station. In this case, a higher CP can be achieved. In detail, we can see that when SS is near the coastline, OSs perform a better CP. When the distance between SS and the

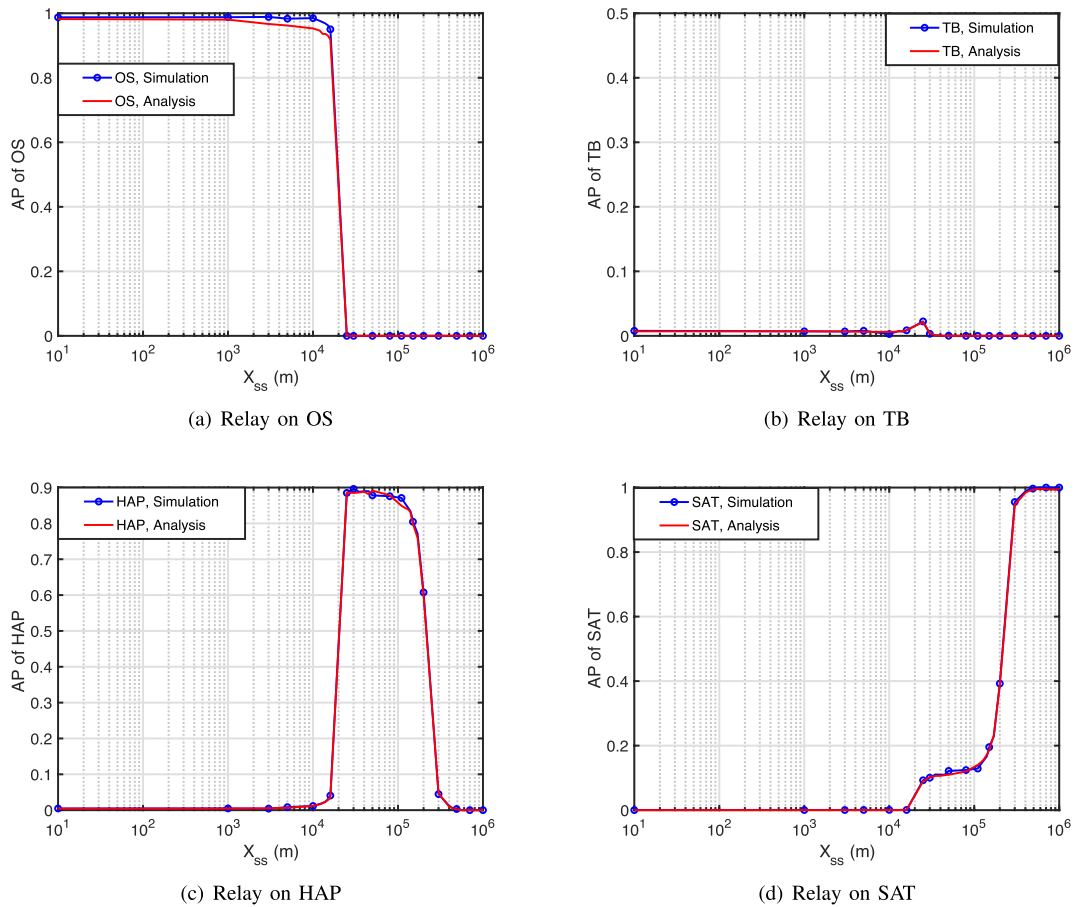


Fig. 7. Association probabilities of four relay stations.

coastline increase, TB, HAP, and SAT will obtain a better CP at different ranges, which shows the potential advantages of SAGSINs.

To decide which type of relay station we should choose in different ranges of X_{ss} , association probabilities of the four different types of relays should be calculated, and they are shown in Fig. 7. Due to the advantage of the minor decay caused by the short communication distance, the OS almost keeps its association probability equal to 1 in the near-shore scenario until the X_{ss} reaches its maximum communication distance, which is shown in Fig. 7(a). Comparing the association probabilities of TB and HAP in Fig. 7(b) and Fig. 7(c), we can find that the association probability of TB is close to zero, but the association probability of HAP is much higher. One of the most important reasons is that the attenuation factor of the TB channel is greater than the HAP channel (they share the same channel model but apply different path loss exponents). So, even though the signal from TB has a shorter communication distance, the received signal’s power at SS from TB is smaller than HAP. As the distance between SS and the coastline increase, the power of the received signal from HAP gradually decreases and turns smaller than the signal received power from SAT. In the communication scenario where SS is far away from the coastline where OS, TB, and HAP are unavailable, the association probability of SAT will reach 1, which is shown in Fig. 7(d).

Fig. 8 shows the advantages of SAGSIN that it can combine the benefits of four different relay stations at different ranges of the distance between SS and the coastline. Firstly, comparing the dashed and solid lines, we can see that the simulation results match the analysis results, which shows the correctness and reliability of the theoretical analysis process in this paper. The two red curves (dashed line and solid line with asterisk) are the total CP of SAGSIN. The lines with different markers, circles, plus signs, diamonds, and crosses, are the analysis CPs of the single relay station, OS, TB, HAP, and SAT, and the four dashed lines with the same color as the marked lines are the four simulation results of CPs of the four different types of single relay station. We can see that most of the time, SAGSIN can integrate the advantages of every single type of relay station and guarantee better performance in an extensive range of X_{ss} , where the distance between SS and the coastline can reach thousands of kilometers.

At the same time, we can also find a trough of CP in Fig. 8 at the point that X_{ss} is near the maximum value of HAP. Checking Fig. 6(c), we can see that during this range of X_{ss} , the CPs of OS and TB are 0, and the CP of HAP is very low (almost 0). According to the association policy in Section II, SS will connect to the relay station with the strongest desired signal power. In this way, the signal power from HAP is higher than the signal power from SAT with a considerable probability, and the A_{hap} is around 0.6, as shown

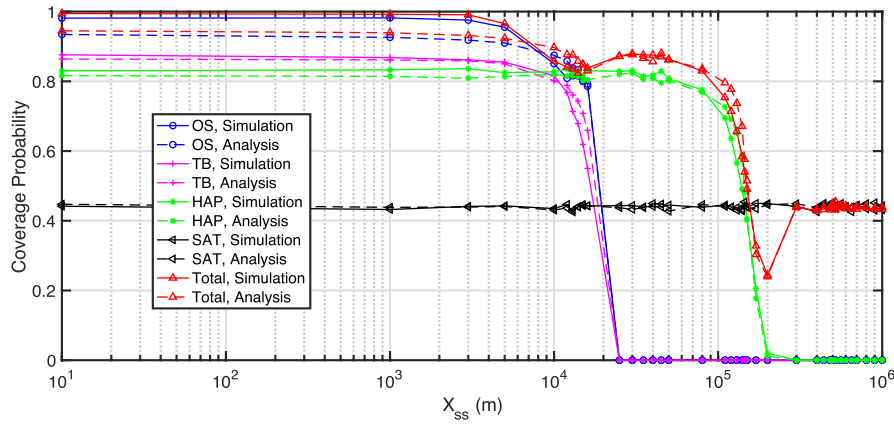


Fig. 8. Comparison of CP of SAGSIN and CP of single relay station.

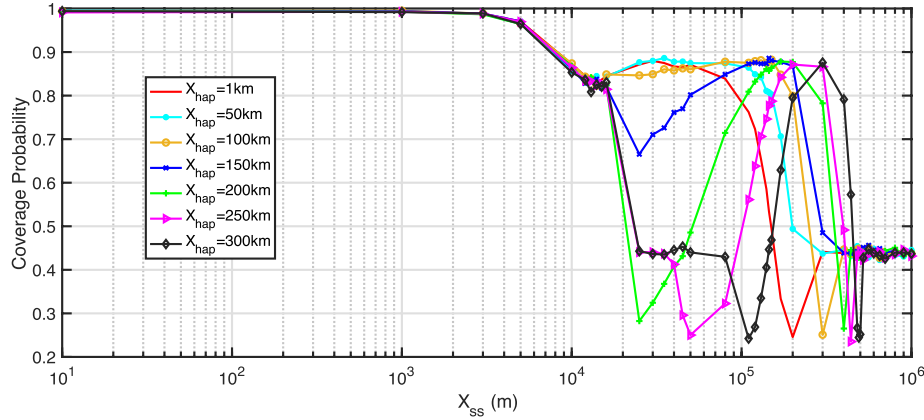


Fig. 9. CPs of SAGSIN with different X_{hap} .

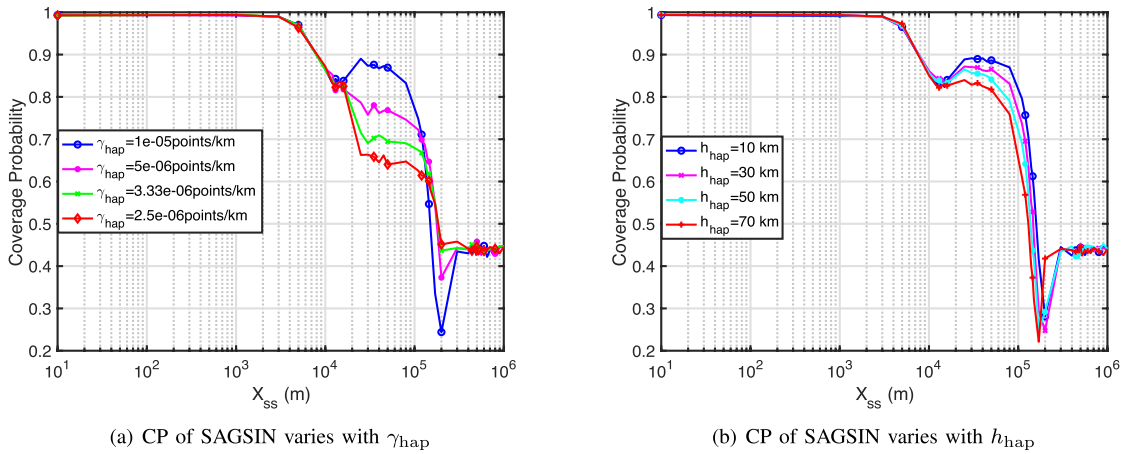


Fig. 10. CP of SAGSIN varies with different parameters.

in Fig. 7(c). However, the SINR of the signal from HAP is low, and the CP of HAP at this condition is almost 0 (as shown in Fig. 6(c)). In a word, when X_{ss} is near the maximum value of HAP, HAPs will have a high association probability but with a low CP, which will result in a low total CP of SAGSIN without an adaptive weight adjustment mechanism. A good way to solve this problem is to optimize the distance between HAP and coastline X_{hap} .

In Fig. 9, the coverage performances with different X_{hap} are revealed. As we can see that when $X_{hap} = 50$ km, the trough

in Fig. 8 can be removed. However, for other values of X_{hap} , we can see that there exists a trough at different values of X_{ss} . This can be resolved by optimizing other system parameters, as discussed later in Fig. 10. There are so many parameters involved in our analysis process, such as densities of OS, TB, and HAP, number of SAT, distances between the coastline and the three relay stations (OS, TB, HAP), heights of OS, TB, and HAP, etc., and we believe all of them can affect the final coverage performance. Here, in Fig. 10, we show how the CP varies with the parameters of γ_{hap} and h_{hap} . In Fig. 10(a),

we can see that the previous trough in Fig. 9 led by the rise of X_{hap} can be fixed at a degree by optimizing the density of HAP, and the trough in Fig. 8 can also be removed with a smaller γ_{hap} . In Fig. 10(b), we can see that the height can also affect the CP of SAGSIN, especially in the range where the HAP is regarded as the main functional relay station. Besides that, in Fig. 10(b), we can see that a higher altitude does not significantly extend the functional range of HAP (the range that HAPs act as the main relay stations). On the contrary, at an altitude of 70 km, the functional range of HAP seemed to decrease. This is reasonable because with the rise of altitude, the communication distance also increases, and the CP of HAP will decrease, which leads to a smaller functional range of HAP.

VI. CONCLUSION

In this work, we proposed a SAGSIN system to improve the CP of SSs over a large-scale and far-reaching ocean surface. OS, TB, HAP, and SAT are designed to assist the communication between CCBS and SSs, and the coverage performance is analyzed. All communication scenarios were presented with practical channel fading assumptions. Taking the random distribution of SSs into consideration, the coverage performance of each link and SAGSIN are analyzed in detail using tools from stochastic geometry. The approximated and asymptotic expression for the CP of each type of relay station was derived, as well as the CP of SAGSIN. After that, according to the analysis results, some insights are revealed to promote the system performance in practical applications and to provide a reference for large-scale and far-reaching maritime communication designers. The correctness of the coverage performance analysis has been verified through Monte-Carlo simulations. Through a comparison of single-relay networks and integrated networks, the superiority of our proposed SAGSIN is revealed.

APPENDIX

A. PDF of the Nearest Distance in 1D-PPP, D_{os}

Based on the theorem of PPP, we can get

$$\begin{aligned} F_{D_{\text{os}}}(d_{\text{os}}) &= \mathbb{P}(D_{\text{os}} \leq d_{\text{os}}) \\ &= \mathbb{P}(\sqrt{(X_{\text{ss}} - X_{\text{os}})^2 + Y_{\text{os}}^2 + (h_{\text{os}} - h_{\text{ss}})^2} \leq d_{\text{os}}) \\ &= \mathbb{P}(0 \leq Y_{\text{os}} \leq \sqrt{d_{\text{os}}^2 - (X_{\text{ss}} - X_{\text{os}})^2 - (h_{\text{os}} - h_{\text{ss}})^2}) \\ &= \int_0^{\sqrt{d_{\text{os}}^2 - (X_{\text{ss}} - X_{\text{os}})^2 - (h_{\text{os}} - h_{\text{ss}})^2}} \gamma_{\text{os}} e^{-\gamma_{\text{os}} y_{\text{os}}} dy_{\text{os}} \\ &= 1 - \exp\left(-\gamma_{\text{os}} \sqrt{d_{\text{os}}^2 - (X_{\text{ss}} - X_{\text{os}})^2 - (h_{\text{os}} - h_{\text{ss}})^2}\right). \end{aligned}$$

Derive $F_{D_{\text{os}}}(d_{\text{os}})$ to get PDF of D_{os} as following.

$$\begin{aligned} f_{D_{\text{os}}}(d_{\text{os}}) &= \frac{\partial F_{D_{\text{os}}}(d_{\text{os}})}{\partial d_{\text{os}}} \\ &= \gamma_{\text{os}} d_{\text{os}} \left(d_{\text{os}}^2 - (X_{\text{ss}} - X_{\text{os}})^2 - (h_{\text{os}} - h_{\text{ss}})^2\right)^{-\frac{1}{2}} \\ &\quad \times \exp\left(-\gamma_{\text{os}} \sqrt{d_{\text{os}}^2 - (X_{\text{ss}} - X_{\text{os}})^2 - (h_{\text{os}} - h_{\text{ss}})^2}\right). \end{aligned}$$

The PDF calculation process of D_{tb} or D_{hap} is very similar to D_{os} , so we do not repeat the derivation.

B. CDF of the Second Nearest Distance With Given the Nearest Distance in 1D-PPP, $F_{D_{\text{os},2}}(d_{\text{os},2}|y_{\text{os}})$

Based on the relationships between y_{os} and $d_{\text{os},2}$, $d_{\text{os},2}$ and $d_{\text{os},2}$ we can get

$$\begin{aligned} F_{D_{\text{os},2}}(d_{\text{os},2}|y_{\text{os}}) &= \mathbb{P}(D_{\text{os},2} < d_{\text{os},2}|y_{\text{os}}) \\ &= \mathbb{P}\left(\sqrt{(X_{\text{ss}} - X_{\text{os}})^2 + Y_{\text{os},2}^2 + (h_{\text{os}} - h_{\text{ss}})^2} < d_{\text{os},2}|y_{\text{os}}\right) \\ &= \mathbb{P}\left(Y_{\text{os},2}^2 < d_{\text{os},2}^2 - (X_{\text{ss}} - X_{\text{os}})^2 - (h_{\text{os}} - h_{\text{ss}})^2|y_{\text{os}}\right) \\ &= \mathbb{P}\left(0 < Y_{\text{os},2} < \sqrt{d_{\text{os},2}^2 - (X_{\text{ss}} - X_{\text{os}})^2 - (h_{\text{os}} - h_{\text{ss}})^2}|y_{\text{os}}\right) \\ &= \int_{y_{\text{os}}}^{\sqrt{d_{\text{os},2}^2 - (X_{\text{ss}} - X_{\text{os}})^2 - (h_{\text{os}} - h_{\text{ss}})^2}} f(y_{\text{os},2}|y_{\text{os}}) dy_{\text{os},2} \\ &= \int_{y_{\text{os}}}^{\sqrt{d_{\text{os},2}^2 - (X_{\text{ss}} - X_{\text{os}})^2 - (h_{\text{os}} - h_{\text{ss}})^2}} \gamma_{\text{os}} \\ &\quad \times \exp(-\gamma_{\text{os}}(y_{\text{os},2} - y_{\text{os}})) dy_{\text{os},2} \\ &= 1 - \exp\left(-\gamma_{\text{os}} \left(\sqrt{d_{\text{os},2}^2 - (X_{\text{ss}} - X_{\text{os}})^2 - (h_{\text{os}} - h_{\text{ss}})^2} - y_{\text{os}}\right)\right). \end{aligned}$$

C. CDF of D_{sat} .

- If $D_{\text{sat}} < h_{\text{sat}}$, we have $\mathbb{P}(D_{\text{sat}} > d_{\text{sat}}) = 1$.
- If $h_{\text{sat}} \leq d_{\text{sat}} \leq d_{\text{sat}}^{\text{max}}$, then we have the contact distance distribution shown at the top of the next page.
- If $d_{\text{sat}} > d_{\text{sat}}^{\text{max}}$, we have

$$\begin{aligned} \mathbb{P}(D_{\text{sat}} > d_{\text{sat}}) &= \mathbb{P}(\text{all the } \varphi \text{ are bigger than } \varphi_{\text{max}}, \varphi_{\text{max}}) \\ &= \arccos\left(\frac{r_e}{r_d}\right) \\ &= \left(\mathbb{P}(\varphi > \arccos\left(\frac{r_e}{r_d}\right))\right)^{n_{\text{sat}}} = \left(1 - \frac{1}{\pi} \arccos\left(\frac{r_e}{r_d}\right)\right)^{n_{\text{sat}}}. \end{aligned}$$

So, we can have $F_{d_{\text{sat}}}(D_{\text{sat}}) = 1 - \mathbb{P}(D_{\text{sat}} > d_{\text{sat}})$.

D. Association Probability of OS

Based on the association policy, we can calculate $A_{\text{os}}(D_{\text{os}})$ as follows.

$$\begin{aligned} A_{\text{os}}(D_{\text{os}}) &= \mathbb{P}\left(C_{\text{r,os}} \mathcal{A}(D_{\text{os}}) > C_{\text{r,tb}} \mathcal{B}(D_{\text{tb}})\right) \\ &\quad \times \mathbb{P}\left(C_{\text{r,os}} \mathcal{A}(D_{\text{os}}) > C_{\text{r,hap}} \mathcal{C}(D_{\text{hap}})\right) \\ &\quad \times \mathbb{P}\left(C_{\text{r,os}} \mathcal{A}(D_{\text{os}}) > C_{\text{r,sat}} \mathcal{D}(D_{\text{sat}})\right) \\ &= \mathbb{P}\left(\mathcal{B}(D_{\text{tb}}) < \frac{C_{\text{r,os}}}{C_{\text{r,tb}}} \mathcal{A}(D_{\text{os}})\right) \mathbb{P}\left(\mathcal{C}(D_{\text{hap}}) < \frac{C_{\text{r,os}}}{C_{\text{r,hap}}} \mathcal{A}(D_{\text{os}})\right) \\ &\quad \times \mathbb{P}\left(\mathcal{D}(D_{\text{sat}}) < \frac{C_{\text{r,os}}}{C_{\text{r,sat}}} \mathcal{A}(D_{\text{os}})\right) \\ &= \int_{d_{\text{tb}}'}^{\infty} \left(\mathbb{1}(d_{\text{tb}} \leq d_{\text{tb}}^{\text{max}}) \mathbb{1}(\mathcal{B}(d_{\text{tb}}) < \frac{C_{\text{r,os}}}{C_{\text{r,tb}}} \mathcal{A}(D_{\text{os}}))\right. \\ &\quad \left. + \mathbb{1}(d_{\text{tb}} > d_{\text{tb}}^{\text{max}})\right) f_{D_{\text{tb}}}(d_{\text{tb}}) dd_{\text{tb}} \end{aligned}$$

$$\begin{aligned}
\mathbb{P}(D_{\text{sat}} > d_{\text{sat}}) &= \mathbb{P}(\text{there is no SAT on the curve of the spherical cap}) \\
&= \left(\mathbb{P}(z_\varphi < z_d) \right)^{n_{\text{sat}}} = \left(\mathbb{P}(r_d \cos(\varphi) < z_d) \right)^{n_{\text{sat}}} \\
&= \left(\mathbb{P}(\varphi > \arccos(\frac{z_d}{r_d}) + \mathbb{P}(\varphi < -\arccos(\frac{z_d}{r_d})) \right)^{n_{\text{sat}}} \\
&= \left(1 - \frac{1}{\pi} \arccos(\frac{z_d}{r_d}) \right)^{n_{\text{sat}}} \\
&= \left(1 - \frac{1}{\pi} \arccos \left(1 - \frac{d_{\text{sat}}^2 - h_{\text{sat}}^2}{2r_e r_d} \right) \right)^{n_{\text{sat}}}.
\end{aligned}$$

$$\begin{aligned}
&\times \int_{d'_{\text{hap}}}^{\infty} \left(\mathbb{1}(d_{\text{hap}} \leq d_{\text{hap}}^{\text{max}}) \mathbb{1}(\mathcal{C}(d_{\text{hap}}) < \frac{C_{r,\text{os}}}{C_{r,\text{hap}}} \mathcal{A}(D_{\text{os}})) \right. \\
&+ \mathbb{1}(d_{\text{hap}} > d_{\text{hap}}^{\text{max}}) \left. \right) f_{D_{\text{hap}}}(d_{\text{hap}}) dd_{\text{hap}} \\
&\times \left(1 - F_{D_{\text{sat}}} \left(\mathcal{D}^{-1} \left(\frac{C_{r,\text{os}}}{C_{r,\text{sat}}} \mathcal{A}(D_{\text{os}}) \right) \right) \right),
\end{aligned}$$

where $d'_{\text{tb}} = \sqrt{(X_{\text{ss}} - X_{\text{tb}})^2 + (h_{\text{ss}} - h_{\text{tb}})^2}$, and $d'_{\text{hap}} = \sqrt{(X_{\text{ss}} - X_{\text{hap}})^2 + (h_{\text{ss}} - h_{\text{hap}})^2}$.

E. CP of OS in the SAGSIN

Based on the association policy, we can calculate $A_{\text{os}}(D_{\text{os}})$ as follows.

$$\begin{aligned}
&\mathbb{E}_{D_{\text{os},2}} \mathbb{E}_{D_{\text{os}}} [A_{\text{os}}(D_{\text{os}}) \mathbb{P}(\text{SINR}_{\text{os}} > \tau | D_{\text{os}}, D_{\text{os},2})] \\
&= \mathbb{E}_{D_{\text{os},2}} \mathbb{E}_{D_{\text{os}}} [A_{\text{os}}(D_{\text{os}}) \\
&\quad \times \mathbb{P}(C_{r,\text{os}} \mathcal{A}(D_{\text{os}}) > \tau (C_{r,\text{os}} \mathcal{A}(D_{\text{os},2}) \\
&\quad + I_{\text{os},3} + \sigma_n^2) | D_{\text{os}}, D_{\text{os},2})].
\end{aligned}$$

Since we have expectation of $I_{\text{os},3}$ as $\mathbb{E}[I_{\text{os},3}] = C_{r,\text{os}} \gamma_{\text{os}} \int_{D_{\text{os},2}}^{d_{\text{os}}^{\text{max}}} \mathcal{A}(x) dx$, so we can have

$$\begin{aligned}
&\mathbb{E}_{D_{\text{os},2}} \mathbb{E}_{D_{\text{os}}} [A_{\text{os}}(D_{\text{os}}) \mathbb{P}(\text{SINR}_{\text{os}} > \tau | D_{\text{os}}, D_{\text{os},2})] \\
&= \mathbb{E}_{D_{\text{os},2}} \mathbb{E}_{D_{\text{os}}} \left[A_{\text{os}}(D_{\text{os}}) \mathbb{P}(\mathcal{A}(D_{\text{os}}) > \tau (\mathcal{A}(D_{\text{os},2}) \right. \\
&\quad \left. + \gamma_{\text{os}} \int_{D_{\text{os},2}}^{d_{\text{os}}^{\text{max}}} \mathcal{A}(x) dx + \frac{\sigma_n^2}{C_{r,\text{os}}}) | D_{\text{os}}, D_{\text{os},2}) \right] \\
&= \int_{\min(d'_{\text{os}}, d_{\text{os}}^{\text{max}})}^{d_{\text{os}}^{\text{max}}} \int_{d_{\text{os}}}^{d_{\text{os}}^{\text{max}}} A_{\text{os}}(d_{\text{os}}) \Xi_{\text{os}}(d_{\text{os},2} | d_{\text{os}}) \\
&\quad \times f_{D_{\text{os},2}}(d_{\text{os},2} | d_{\text{os}}) dd_{\text{os},2} f_{D_{\text{os}}}(d_{\text{os}}) dd_{\text{os}},
\end{aligned}$$

where $d'_{\text{os}} = \sqrt{(X_{\text{ss}} - X_{\text{os}})^2 + (h_{\text{ss}} - h_{\text{os}})^2}$, $A_{\text{os}}(d_{\text{os}})$ is shown in (28), and

$$\begin{aligned}
&\Xi_{\text{os}}(d_{\text{os},2} | d_{\text{os}}) \\
&= \mathbb{1} \left(\mathcal{A}(d_{\text{os}}) > \tau (\mathcal{A}(d_{\text{os},2}) + \gamma_{\text{os}} \int_{d_{\text{os},2}}^{d_{\text{os}}^{\text{max}}} \mathcal{A}(x) dx + \frac{\sigma_n^2}{C_{r,\text{os}}}) \right).
\end{aligned}$$

REFERENCES

- [1] J. Liu, Y. Shi, Z. M. Fadlullah, and N. Kato, "Space-air-ground integrated network: A survey," *IEEE Commun. Surveys Tuts.*, vol. 20, no. 4, pp. 2714–2741, 4th Quart., 2018.
- [2] W. Khawaja, I. Guvenc, D. W. Matolak, U. Fiebig, and N. Schneckenburger, "A survey of air-to-ground propagation channel modeling for unmanned aerial vehicles," *IEEE Commun. Surveys Tuts.*, vol. 21, no. 3, pp. 2361–2391, 3rd Quart., 2019.
- [3] N. Kato et al., "Optimizing space-air-ground integrated networks by artificial intelligence," *IEEE Wireless Commun.*, vol. 26, no. 4, pp. 140–147, Aug. 2019.
- [4] N. Cheng et al., "A comprehensive simulation platform for space-air-ground integrated network," *IEEE Wireless Commun.*, vol. 27, no. 1, pp. 178–185, Feb. 2020.
- [5] H. Guo, J. Li, J. Liu, N. Tian, and N. Kato, "A survey on space-air-ground-sea integrated network security in 6G," *IEEE Commun. Surveys Tuts.*, vol. 24, no. 1, pp. 53–87, 1st Quart., 2022.
- [6] Z. Zhang et al., "6G wireless networks: Vision, requirements, architecture, and key technologies," *IEEE Veh. Technol. Mag.*, vol. 14, no. 3, pp. 28–41, Sep. 2019.
- [7] J.-H. Lee, J. Choi, W.-H. Lee, J.-W. Choi, and S.-C. Kim, "Measurement and analysis on land-to-ship offshore wireless channel in 2.4 GHz," *IEEE Wireless Commun. Lett.*, vol. 6, no. 2, pp. 222–225, Apr. 2017.
- [8] Y. H. Lee, F. Dong, and Y. S. Meng, "Near sea-surface mobile radiowave propagation at 5 GHz: Measurements and modeling," *Radioengineering*, vol. 23, no. 3, pp. 824–830, Sep. 2014.
- [9] T. Wei, W. Feng, Y. Chen, C.-X. Wang, N. Ge, and J. Lu, "Hybrid satellite-terrestrial communication networks for the maritime Internet of Things: Key technologies, opportunities, and challenges," *IEEE Internet Things J.*, vol. 8, no. 11, pp. 8910–8934, Jun. 2021.
- [10] X. Li, W. Feng, Y. Chen, C.-X. Wang, and N. Ge, "Maritime coverage enhancement using UAVs coordinated with hybrid satellite-terrestrial networks," *IEEE Trans. Commun.*, vol. 68, no. 4, pp. 2355–2369, Apr. 2020.
- [11] J. Xu, M. A. Kishk, and M.-S. Alouini, "Coverage enhancement of underwater Internet of Things using multilevel acoustic communication networks," *IEEE Internet Things J.*, vol. 9, no. 24, pp. 25373–25385, Dec. 2022.
- [12] J. Yang, J. Wen, Y. Wang, B. Jiang, H. Wang, and H. Song, "Fog-based marine environmental information monitoring toward ocean of things," *IEEE Internet Things J.*, vol. 7, no. 5, pp. 4238–4247, May 2020.
- [13] P. W. Kimball and S. M. Rock, "Mapping of translating, rotating icebergs with an autonomous underwater vehicle," *IEEE J. Ocean. Eng.*, vol. 40, no. 1, pp. 196–208, Jan. 2014.
- [14] H. Ghafoor and Y. Noh, "An overview of next-generation underwater target detection and tracking: An integrated underwater architecture," *IEEE Access*, vol. 7, pp. 98841–98853, 2019.
- [15] F. Besson et al., "A centralized web-based platform for combined glider and satellite observation analysis," in *Proc. OCEANS*, Marseille, 2019, pp. 1–5.
- [16] C. Qin, J. Du, J. Wang, and Y. Ren, "A hierarchical information acquisition system for AUV assisted Internet of underwater things," *IEEE Access*, vol. 8, pp. 176089–176100, 2020.
- [17] T. Matsuda, T. Maki, Y. Sato, and T. Sakamaki, "Experimental evaluation of accuracy and efficiency of alternating landmark navigation by multiple AUVs," *IEEE J. Ocean. Eng.*, vol. 43, no. 2, pp. 288–310, Apr. 2018.
- [18] C. Lin, G. Han, J. Du, Y. Bi, L. Shu, and K. Fan, "A path planning scheme for AUV flock-based Internet-of-Underwater-things systems to enable transparent and smart ocean," *IEEE Internet Things J.*, vol. 7, no. 10, pp. 9760–9772, Oct. 2020.

- [19] J. Du, C. Jiang, J. Wang, Y. Ren, and M. Debbah, "Machine learning for 6G wireless networks: Carrying forward enhanced bandwidth, massive access, and ultrareliable/low-latency service," *IEEE Veh. Technol. Mag.*, vol. 15, no. 4, pp. 122–134, Dec. 2020.
- [20] Z. Niu, X. S. Shen, Q. Zhang, and Y. Tang, "Space-air-ground integrated vehicular network for connected and automated vehicles: Challenges and solutions," *Intell. Converged Netw.*, vol. 1, no. 2, pp. 142–169, Sep. 2020.
- [21] T. Yang et al., "Multi-armed bandits learning for task offloading in maritime edge intelligence networks," *IEEE Trans. Veh. Technol.*, vol. 71, no. 4, pp. 4212–4224, Apr. 2022.
- [22] S. Wen, P.-Y. Kong, J. Shankar, H. Wang, Y. Ge, and C.-W. Ang, "A novel framework to simulate maritime wireless communication networks," in *Proc. OCEANS*, Sep. 2007, pp. 1–6.
- [23] K. Yang, T. Roste, F. Bekkadal, and T. Ekman, "Experimental multipath delay profile of mobile radio channels over sea at 2 GHz," in *Proc. Loughborough Antennas Propag. Conf. (LAPC)*, Nov. 2012, pp. 1–4.
- [24] S. N. Rao, D. Raj, V. Parthasarathy, S. Aiswarya, M. V. Ramesh, and V. Rangan, "A novel solution for high speed internet over the oceans," in *Proc. IEEE Conf. Comput. Commun. Workshops (INFOCOM WKSHPS)*, Apr. 2018, pp. 906–912.
- [25] J. Du, J. Song, Y. Ren, and J. Wang, "Convergence of broadband and broadcast/multicast in maritime information networks," *Tsinghua Sci. Technol.*, vol. 26, no. 5, pp. 592–607, Oct. 2021.
- [26] J. Zhang, F. Liang, B. Li, Z. Yang, Y. Wu, and H. Zhu, "Placement optimization of caching UAV-assisted mobile relay maritime communication," *China Commun.*, vol. 17, no. 8, pp. 209–219, Aug. 2020.
- [27] F. B. Teixeira, R. Campos, and M. Ricardo, "Height optimization in aerial networks for enhanced broadband communications at sea," *IEEE Access*, vol. 8, pp. 28311–28323, 2020.
- [28] T. A. Johansen, A. Zolich, T. Hansen, and A. J. Sorensen, "Unmanned aerial vehicle as communication relay for autonomous underwater vehicle—Field tests," in *Proc. IEEE Globecom Workshops (GC Wkshps)*, Dec. 2014, pp. 1469–1474.
- [29] Y. Yasuda, M. Ohashi, F. Sugaya, M. Yasunaga, and Y. Karasawa, "Field experiment on digital maritime and aeronautical satellite communication systems using ETS-V," in *Proc. IEEE Int. Conf. Commun., World Prosperity Through Commun.*, vol. 1, Jun. 1989, pp. 204–210.
- [30] F. Wei, B. Chen, R. Jia, T. Wang, and L. Wang, "Research on maritime leapfrog emergency communication coverage technology based on satellite relay," *J. Phys., Conf.*, vol. 1087, Sep. 2018, Art. no. 042064.
- [31] T. Aoyagi, K. Suzuki, Y. Suzuki, T. Hirose, and T. Sugiyama, "Wave propagation simulations for considering the installation of the maritime mobile satellite communication antennas," in *Proc. Asia Pacific Microw. Conf. Proc.*, Dec. 2012, pp. 346–348.
- [32] L. Arienzo, "Green RF/FSO communications in cognitive relay-based space information networks for maritime surveillance," *IEEE Trans. Cognit. Commun. Netw.*, vol. 5, no. 4, pp. 1182–1193, Dec. 2019.
- [33] T. Xia, M. M. Wang, and X. You, "Satellite machine-type communication for maritime Internet of Things: An interference perspective," *IEEE Access*, vol. 7, pp. 76404–76415, 2019.
- [34] J. P. Dhivvy, S. N. Rao, and S. Simi, "Towards maximizing throughput and coverage of a novel heterogeneous maritime communication network," in *Proc. 18th ACM Int. Symp. Mobile Ad Hoc Netw. Comput.*, Jul. 2017, pp. 1–2.
- [35] T. Xia, M. M. Wang, J. Zhang, and L. Wang, "Maritime Internet of Things: Challenges and solutions," *IEEE Wireless Commun.*, vol. 27, no. 2, pp. 188–196, Apr. 2020.
- [36] *P.1546: Method for Point-to-Area Predictions for Terrestrial Services in the Frequency Range 30 MHz to 4000 MHz*. Accessed: Nov. 20, 2021. [Online]. Available: <https://www.itu.int/rec/R-REC-P.1546/en>
- [37] A. Talgat, M. A. Kishk, and M.-S. Alouini, "Stochastic geometry-based analysis of LEO satellite communication systems," *IEEE Commun. Lett.*, vol. 25, no. 8, pp. 2458–2462, Aug. 2020.
- [38] V. Garg, *Wireless Communications & Networking*. Amsterdam, The Netherlands: Elsevier, 2010.
- [39] J. G. Andrews, A. K. Gupta, and H. S. Dhillon, "A primer on cellular network analysis using stochastic geometry," 2016, *arXiv:1604.03183*.
- [40] D. Molchanov, "Distance distributions in random networks," *Ad Hoc Netw.*, vol. 10, no. 6, pp. 1146–1166, Aug. 2012.
- [41] W. Wang, Y. Tong, L. Li, A.-A. Lu, L. You, and X. Gao, "Near optimal timing and frequency offset estimation for 5G integrated leo satellite communication system," *IEEE Access*, vol. 7, pp. 113298–113310, 2019.
- [42] Y. Zhang, Y. Wu, A. Liu, X. Xia, T. Pan, and X. Liu, "Deep learning-based channel prediction for LEO satellite massive MIMO communication system," *IEEE Wireless Commun. Lett.*, vol. 10, no. 8, pp. 1835–1839, Aug. 2021.
- [43] A. Talgat, M. A. Kishk, and M.-S. Alouini, "Nearest neighbor and contact distance distribution for binomial point process on spherical surfaces," *IEEE Commun. Lett.*, vol. 24, no. 12, pp. 2659–2663, Dec. 2020.
- [44] S. A. Khaleefa, S. H. Alsamhi, and N. S. Rajput, "Tethered balloon technology for telecommunication, coverage and path loss," in *Proc. IEEE Students' Conf. Electr., Electron. Comput. Sci.*, Mar. 2014, pp. 1–4.
- [45] G. Mingxiang, Y. Fang, and G. Qing, "Performance of coverage and wireless link for HAPS communication," in *Proc. Int. Conf. Wireless Commun. Signal Process.*, Nov. 2009, pp. 1–4.



Jiajie Xu (Graduate Student Member, IEEE) received the B.Sc. degree from Lanzhou Jiaotong University, Lanzhou, China, in 2016, and the M.Sc. degree from Yanshan University, Qinhuangdao, China, in 2019. He is currently pursuing the Ph.D. degree with the Communication Theory Laboratory, King Abdullah University of Science and Technology, Thuwal, Saudi Arabia. His current research interests include underwater wireless acoustic communication, underwater target detection, underwater cooperative networks, maritime communication, and communication systems, stochastic geometry, and energy harvesting wireless networks.



Mustafa A. Kishk (Member, IEEE) received the B.Sc. and M.Sc. degrees in electrical engineering from Cairo University, Giza, Egypt, in 2013 and 2015, respectively, and the Ph.D. degree in electrical engineering from Virginia Tech, Blacksburg, VA, USA, in 2018. He is currently an Assistant Professor with the Department of Electronic Engineering, Maynooth University, Ireland. Before that, he was a Post-Doctoral Research Fellow with the Communication Theory Laboratory, King Abdullah University of Science and Technology, Saudi Arabia. His current research interests include stochastic geometry, UAV-enabled communication systems, and satellite-enabled communications. He was a recipient of the IEEE ComSoc Outstanding Young Researcher Award for Europe, Middle East, and Africa Region, in 2022. He was recognized as an Exemplary Reviewer by the IEEE COMMUNICATIONS LETTERS in 2020. He serves as an Associate Editor for the IEEE WIRELESS COMMUNICATION LETTERS.



Mohamed-Slim Alouini (Fellow, IEEE) was born in Tunis, Tunisia. He received the Ph.D. degree in electrical engineering from the California Institute of Technology (Caltech), Pasadena, CA, USA, in 1998. He was a Faculty Member at the University of Minnesota, then at Texas A&M University at Qatar, before joining the King Abdullah University of Science and Technology (KAUST) in 2009, where he is currently a Distinguished Professor of electrical and computer engineering. He is a fellow of OSA. He is particularly interested in addressing the technical challenges associated with the uneven distribution, access to, and use of information and communication technologies in far-flung, rural, low-density populations, low-income, and/or hard-to-reach areas.